Applied Energy 380 (2025) 124952

Contents lists available at ScienceDirect

Applied Energy

journal homepage: www.elsevier.com/locate/apenergy

Development of integrated energy sharing systems between neighboring zero-energy buildings via micro-grid and local electric vehicles with energy trading business models

Suijie Liu [a], Sunliang Cao [a,b,c,*]

[a] Renewable Energy Research Group (RERG), Department of Building Environment and Energy Engineering, Faculty of Construction and Environment, The Hong Kong Polytechnic University, Kowloon, Hong Kong Special Administrative Region

[b] Research Institute for Smart Energy (RISE), The Hong Kong Polytechnic University, Kowloon, Hong Kong Special Administrative Region

[c] Research Institute for Sustainable Urban Development (RISUD), The Hong Kong Polytechnic University, Kowloon, Hong Kong Special Administrative Region

HIGHLIGHTS

- Integrated building energy sharing systems via micro-grid and electric vehicles.
- Energy trading business models for both the external and local grid-tied ZEBs.
- Energy management of renewable, grid and storage resources between nearby ZEBs.
- Integrated energy sharing systems between neighboring zero-energy buildings.
- Techno-economic impact of novel energy trading models between neighboring ZEBs.

ARTICLE INFO

Keywords:
Integrated energy-sharing system
Grid-tied zero-energy buildings
Energy-trading business models
Micro-grid sharing
Energy management

ABSTRACT

Applying high-efficient combinations of renewable energy systems and effective energy management of renewables, grid and storage resources between neighboring grid-tied zero-energy buildings (ZEB) has become growingly significant to improve the techno-economic performance of hybrid building systems. However, majority of the existed research mainly analyzed one single energy-sharing method based on simple technical yearly index. The techno-economic impact evaluated by matching index (WMI) and net present value (NPV) of various hybrid renewable energy systems combined with three different integrated building energy-sharing systems via instantaneous and predictive micro-grid-based, and local electric-vehicle(EV)-based energy-sharing remains uncovered. The research results show that with integration of instantaneous micro-grid-based and local-EV-based energy-sharing system, the techno-economic performance is enhanced (average WMI improved by 7.19 % and 6.86 %, NPV improved by 9.53 % and 5.70 %, respectively), while specific cases show various improvement outcomes largely related to the types of renewable combinations. Under instantaneous micro-grid-based sharing, the divergency of two buildings' renewable combinations brings at most 33.59 % technical improvement and 3,764,380 HKD economic benefits. In contrast, the similarity of both renewable combinations helps achieve a maximum 12.02 % matching enhancement and an extra 866,690HKD NPV improvement under local EV-based energy-sharing. As for the common energy trading business model, the building with more energy shared earns more profits as the trading price increases. However, when the residence is under the "Predictive Micro-grid-based Energy-Sharing Control" mode, a lower trading price below 0.5 HKD of the specific case is more likely to minimize the loss of office stakeholder as well as maintain positive profits of residence owners.

1. Introduction and background

Nowadays, the topic of carbon neutrality has become increasingly important under the background of climate change and global warming. In Hong Kong, the building and transportation sectors have contributed 95 % of the final total energy consumption compared to the world average of 50 % due to its highly developed urbanization and industry

* Corresponding author at: Renewable Energy Research Group (RERG), Department of Building Environment and Energy Engineering, Faculty of Construction and Environment, The Hong Kong Polytechnic University, Kowloon, Hong Kong Special Administrative Region

E-mail addresses: sunliang.cao@polyu.edu.hk, caosunliang@msn.com (S. Cao).

https://doi.org/10.1016/j.apenergy.2024.124952
Received 25 July 2024; Received in revised form 11 September 2024; Accepted 16 November 2024
Available online 6 December 2024

Nomenclature

ZEB	Zero-energy building
PV	Photovoltaic system
BIPV	Building integrated photovoltaic system
FPV	Floating photovoltaic system
WT	Wind turbine
REe	Renewable electricity
EV	Electric vehicle
B2V	Building-to-vehicle energy interaction
V2B	Vehicle-to-building energy interaction
DHW	Domestic hot water
AHU	Air handling unit
P_{REe}	Renewable electricity generation power (kW)
P_{imp}	Imported power from the external grid (kW)
P_{exp}	Exported power to the external grid (kW)
P_{B2V}	Charging power from building to electric vehicle (kW)
P_{V2B}	Discharging power from electric vehicle to building (kW)
P_{O2R_MG}	Sharing power from office to residence by micro-grid (kW)
P_{R2O_MG}	Sharing power from residence to office by micro-grid (kW)
Gen_{OffRe}	Office renewable energy generation
Gen_{ResRe}	Residence renewable energy generation
Gap_{Off}	Office energy gap between renewable energy generation and building demand
Gap_{Res}	Residence energy gap between renewable energy generation and building demand
CH_{OEV}	Office electric vehicle charging energy amount
CH_{REV}	Residential electric vehicle charging energy amount
CH_{RB}	Residential building battery charging energy amount
MG_{O2R}	Shared energy amount by micro-grid from office to residence
MG_{R2O}	Shared energy amount by micro-grid from residence to office
$DisCH_{OEV}$	Office electric vehicle discharging energy amount
$DisCH_{REV}$	Residential electric vehicle discharging energy amount
$E_{Offimp.a}$	Annual office energy import amount
$E_{Resimp.a}$	Annual residence energy import amount
$E_{Offexp.a}$	Annual office energy export amount
$E_{Resexp.a}$	Annual residence energy export amount
MCM	Mandatory charging mode
FSOC	Fractional state of charge
OEFe	On-site electrical energy fraction
OEMe	On-site electrical energy matching
WMI	Weighting matching index
LEV	Local electric vehicle
E_{B2V}	Electricity transferred from building to electric vehicle (kWh)
E_{V2B}	Electricity transferred from electric vehicle to building (kWh)
E_{O2R_MG}	Electricity shared from office to residence by micro-grid (kWh)
E_{R2O_MG}	Electricity shared from residence to office by micro-grid (kWh)
E_{O2R_LEV}	Electricity shared from office to residence by local electric vehicle (kWh)
E_{R2O_LEV}	Electricity shared from residence to office by local electric vehicle (kWh)
NPV	Net present value
HKD	Hong Kong dollar
MG	Micro-grid
DMI	Decision-making index
DMI_R	Decision-making index of residence
OEV	Office electric vehicle
REV	Residential electric vehicle

structure, resulting in a large amount of carbon emission [1]. The HKSAR Government has announced that the carbon neutrality deadline is 2050, while the mid-term carbon emissions target is set for a 50 % reduction before 2035 compared to 2005 [2]. Regarding the high proportion of carbon emissions resulted from energy consumption in the building and transportation sectors in Hong Kong, it is essential to reduce the energy consumption of these two sectors comprehensively.

In the academic field, in order to achieve building sector energy consumption reduction, many researchers are focusing on the zero-energy building (ZEB) technologies as a promising solution to cut down the building energy consumption as well as accelerating the decarbonization process [3–6]. There are several different definitions of ZEB in the academic world [7]. In this study, ZEB is defined as a building whose self-renewables generation equals or is larger than its energy demand in one year [7] [8]. According to the research review of Ahmed and his colleagues, renewable energy can be categorized into two parts based on the supply location (e.g. on-site and off-site) and mainly comes from hydropower, wind energy and solar energy. Hydropower generation is greatly restricted by geographical factors and is mainly used at the power plant side of the grid instead of the building demand side [9]. Photovoltaic panels (PV) and wind turbines are typical technologies to utilize solar and wind energy respectively at the building demand side [10,11]. PVs are usually installed in a building-integrated way on top of the roof or mounted to the facades in ZEBs in the case of on-site production [12]. Some researched ZEBs close to the seashore adopt floating photovoltaics (FPV) technologies to utilize more water surfaces for off-site solar energy [13]. Different renewable electricity (REe) combinations impact greatly the technical and economic outcome of building hybrid systems. Luo and his team [14] studied the techno-economic performance improvement of on-shore roof-top PV installations of different levels of homestay hotels in Hainan Province in China, showing that the integration of roof PVs can cover up to 63.87 % of energy consumption and achieve maximum 31.4 % of profit increase, making it technically and financially feasible to invest on PV system. Similar results have also been noticed by the study of Fabian and his team [15] of the Kenyan institutional building, which the institutional building is found to achieve approximately 77 % reduction in power grid importation and 84 % less electricity bill when installed on-shore PVs and wind turbines can cover 71.6 % of the total electricity demand [15,16]. According to the existing research of Haojie and Sunliang, with off-shore hybrid wind-wave energy generation systems (62 % wave generation and 38 % wind generation), the coastal zero-energy building can save imported electricity that is partially generated by fossil energy by 69 %, therefore reducing the carbon emissions at the power plant side [16]. Qiang Gao's research investigated the combination of wind and wave generation in a power plant can dramatically bring up to a 20 % increase in power capacity and a maximum of 35 % improvement in energy capacity compared to the sole wind-supported power plant [17]. Inother words, the saving storage capacity also leads to lower capital investment, making positive financial feedback of renewable energy systems investment feasible [17]. As a result of the unstable nature of renewable energy (e.g., solar and wind energy), ZEB still needs to have frequent interactions with the electric grid. Still, it reduces reliance on the power grid side [18]. Some similar studies on the impact of different REe systems of ZEB are also available in the references of Luo et al. [19], Abdou et al. [20], Krarti et al. [21], and Tumminia et al. [22].

Meantime, an unstoppable trend of electric vehicle (EV) penetration can be observed in the transportation sector in Hong Kong [23], resulting in increasingly high interactions between the building and transportation sectors. Though we consider the EVs won't emit any CO_2 on the roadside, the equivalent carbon emissions are transferred to the building side especially when EVs are charged in the building via the "Building-to-Vehicle (B2V)" function. Therefore, reducing the corresponding carbon emissions of the building sector will also become a challenge. The results of Madeline Gilleran's research on investigating the impact of the EV public retail building charging (B2V only) in the US showed that fast charging would bring a significant increase of more than 250 % on on-site peak power demand in some cases, leading to a stressful pressure on the power grid side [24]. This phenomenon became more serious when per-port charging power levels rose. Moreover, the capacity issues frequently occur due to the overlapping of charging ports demand and the existing building demand. In addition, Madeline et al. also pointed out that if the charging loads correspond with rate structures incorporating high demand charges fees, the annual electricity bill is susceptible to increase up to 88 % [24]. Similar EV charging demand increase has also been observed by Stefano Bracco. The results of their research showed that by the renewable generation from PVs and wind turbines, the impact on the grid by B2V charging can be alleviated, therefore resulting in the reduced amount of imported electricity from the external grid and lower electricity bills [25]. Meanwhile, except for the abovementioned B2V impact research, more researchers have turned their attention to the interactions of Vehicle-to-Building (V2B) which the EV batteries are utilized as movable energy storages for buildings. A research team led by Liu investigated the potential ability of EVs as mobile energy storage devices to reduce load differences between peak and valley hours [26]. Ahmed Ouammi investigated that by integrating V2B functions with the building micro-grid, the discharging electricity from EVs can successfully achieve peak load reduction of one solar PV-supported building. The results of his research also revealed that utilizing the operational flexibilities of EVs' participation in shaving the building peak load is helpful to handle the uncertainties of the renewable generation nature [27]. Liu's team studied a techno-economic analysis on V2B interaction in zero-energy building. Their results turned out that introducing EV discharge improves 2.6 % on renewable utilization ratio,12.1 % on load matching ratio, and reduces 18.7 % on electricity bills as well as 6.2 % on levelized energy costs [28]. Other similar research on the V2B impact on building hybrid systems can be located in the following references authored by Li et al. [8], Zou [29], David et al. [30], Lo et al. [31], He et al. [32], and Mahdi et al. [33].

There have been recent studies that focused on various kinds of energy sharing of buildings. Pei Huang's research on renewable PV power sharing between three neighboring buildings using a micro-grid showed that sharing electricity as an aggregated cluster helps the buildings to achieve the same level of system performance with a smaller PV installation capacity compared to no sharing due to the enhanced matching capability and improved building self-consumption rate [34]. Some researchers focused on the interactions between the EVs and the buildings by B2V and V2B function. According to David Borge-Diez et al. results, integration owned EVs sharing by V2B strategies can transform the EVs into mobile energy storages without any extra investments. The V2B sharing functions reduce the building peak demand by 50 %, which leads to multiple benefits including grid impact reduction, increasing utilization of EVs, higher renewable energy sharing and economic profits. It illustrates that it is meaningful to include the V2B application of EVs in building energy management structures for more energy flexibility [30]. Moreover, the technical and economic feasibility of 22 European cities with the Building-To-Vehicle-To-Building scheme was studied by Giovanni Barone and his colleagues. From a technical perspective, the building electricity importation reductions from the power grid range from 13 % to 71 %. Some cases show great potential for profits with a net present value of up to 18.1 k€ due to the building location with a high level of solar intensity and beneficial electricity price [35]. Some similar results have also been confirmed from the studies of Cao that there are some matching capabilities enhancement by purely activating the V2B function. However, the scale of matching capabilities enhancement between buildings is largely affected by the relationship between the time of renewable energy surplus, the EVs' parking schedule and the vehicle energy consumption [36]. Some researchers like Kumari's team focused on the technical application of energy sharing using decentralized and transparent P2P energy trading schemes based on blockchain. It demonstrated that adopting a dynamic trading price is beneficial for both consumers and prosumers [37]. It also indicated that the further updated trading scheme has the potential to resolve the security and privacy issues, pointing out a feasible technical solution for building energy-sharing applications [38].

Drawing from the literature reviews previously mentioned above, it is noticeable that the following scientific gaps exist in the academic world:

Firstly, the existing academic research mainly focused on the technical and economic performance of one individual building with one type of REe such as PV or different REe combinations such as on-shore (PV and wind turbine) or off-shore (Wave generator and wind turbine) [15–17,39]. There is little detailed investigation of two separate ZEBs based on the technical and economic performance with both on-shore (PV and wind turbine) and off-shore (FPV) renewables combinations. Most past studies used simple yearly index, for example, the annual electricity bill to evaluate the economic performance [15,17,39]. Seldom studies considered the investment cost and profit return of the hybrid renewable system in a long-term base using net present value index. How the on-shore PV and wind turbine and off-shore FPV impact the technical and economic performance of two separated hybrid building systems is an attractive question remains uncovered.

Secondly, when the ZEB possessed the function of B2V and V2B, researchers like Liu et al. [28] and David Borge-Diez et al. [30] mainly analyzed the interaction between the EVs and one building. The interactions between the EVs and two neighboring buildings with different renewable combinations are still unknown, especially on how the differences in building renewable energy systems will affect the performance of two ZEBs with V2B functions. Furthermore, seldom research has been concentrated on the impact of the different schedules of EVs owned by different types of buildings. The EVs owned by different types of buildings have different usage patterns and parking schedules, therefore will largely impact the building-to-vehicle-to-building interactions outcome when the stakeholders use the EVs as mobile energy storages.

Thirdly, building on the initial point discussed, there has not been any research dedicated to examining the technical and economic aspects (such as grid interaction, investment and operational costs, net present value, etc.) of various energy sharing approaches (like instantaneous and predictive micro-grid-based and local EV-based energy-sharing) across two building types (residence and office). Most studies mainly focused on only one type of integrated energy-sharing method such as micro-grid conducted by Pei Huang et al. [34] and EV sharing conducted by David Borge-Diez et al. [30] and Giovanni Barone et al. [35]. For the micro-grid sharing method, very limited studies were investigating the energy interactions between different kinds of buildings with various operation patterns. For the EV sharing method, most existing studies were about the interactions between one building and EVs. How EV sharing will affect two buildings' performance remains an appealing topic. Moreover, most previous research studied building energy-sharing owned by the same stakeholder. There are very few studies focusing on energy sharing and trading between two neighboring buildings belonging to two different stakeholders, making the understanding of the influence of different sharing methods a worthwhile research objective.

This paper addresses the abovementioned three identified scientific gaps by examining a residential and an office zero-energy building. These buildings are supported by diverse combinations of hybrid on-shore BIPVs, wind turbines, and off-shore floating PV renewable energy systems, each owned by two stakeholders. The contributions of this paper are listed below:

The first contribution of this paper is to provide a detailed technical and economic analysis using some comprehensive index such as net present value to evaluate the impact of investment cost and profit return of both on-shore and off-shore renewable energy systems.

The second contribution is to demonstrate the interactions and performance influence of different building renewable energy systems and distinct EV schedules on two different types of neighboring buildings.

The third contribution is that it illustrated the technical and economic performance of various kinds of energy-sharing controls between two different types of buildings with diverse operation patterns based on multi-objective indexes. The research also revealed the financial impact on energy trading with different building stakeholders.

The following Section 2 of this paper will present the weather conditions, building demands, and the simulation environment. This will be followed in Section 3 by detailed descriptions of the building services, energy system control strategies, and renewable energy systems. Section 4 will delineate the analytical criteria, while Section 5 will present the simulation outcomes, accompanied by comprehensive evaluation, analyses and discussions. Finally, the conclusions of this study will be delineated in Section 6.

2. Weather, building demands, and methodology

The studied two buildings are both coastal buildings in Hong Kong, which are located in the southern part of China within subtropical climate zones. These two buildings are neighboring buildings, for one is an office building, and the other is a residential building. The mixture of different building types like offices and residences is commonly seen in Hong Kong suburban areas such as Chai Wan, Repulse Bay, Stanley, etc. The weather file comprises hourly data on temperature, humidity ratio, wind speed, and solar radiation, all of which are critical inputs for building energy simulations. Utilizing Metronome weather data specific to Hong Kong, it is noted that the annual total solar radiation on a horizontal surface amounts to 1423 kWh/m^2. Fig. 1 further depicts both the total horizontal solar radiation and the average wind speeds for twelve months. The peak solar radiation is observed in July, reaching 168.5 kWh/m^2, while the minimum occurs in February, at 63.9 kWh/m^2, reflecting the typical summer-winter cycle characteristic of the subtropical zone in China. Relatively more stable wind speed can be observed at around 4.6–5.7 m/s in whole year except for July at 3.6 m/s.

The simulation of the floating photovoltaic (FPV) system incorporated seawater temperature data obtained from the Hong Kong Observatory. Based on this data, the average seawater temperature in Hong Kong ranges from 16.20 $^{\circ}C$ to 29.55 $^{\circ}C$, with an annual average value reaching 22.90 $^{\circ}C$, showing much stable temperature fluctuation compared to the air.

The studied office and residential buildings are set to be owned by two different stakeholders, with the same layout with 5 floors above ground. Each floor was in a 20m × 20m rectangular shape with a 3-m floor height. The architectural design of the building envelopes, insulation, service systems, and operational schedules were all developed following the Performance-based Building Energy Code of Hong Kong [40] as listed in Appendix A. The window-to-wall ratio of the external facade was established at 0.21 to prevent unnecessary solar heat gain through glazing in alignment with recommendations from the Hong Kong Green Office Guide [41]. The total energy demand and the peak power demand in one year of building services systems such as the different cooling and heating systems, domestic hot water (DHW) heating as well as the building electricity demand exclusive of any energy-conserving strategies and REe generation system of each building were illustrated in Table 1 and Table 2. Fig. 2 presents their duration curves of one year, respectively. The electric demands including illumination, equipment operation and ventilation fan usage are presented in Table 1, Table 2 and Fig. 2, excluding the contributions from the buildings' cooling and heating systems.

Each building has one local electric vehicle (EV) owned by each stakeholder and one charging pile on its ground floor, respectively. For the EV owned by the office building, it is assumed that the office EV parks at the office building during the period of 0:00–8:00, and 18:00–24:00 and stays in the residential building from 11:00–16:00 on weekdays. At 8:00 and 16:00 from Monday to Friday, the office EV will go on a 3-h (30 km), and 2-h (20 km) business trip, respectively. During the weekend, the office EV remains parked in the office. As for the residential EV, it is scheduled to park in the residential building from 20:00 to 8:00 on the next morning and park in the office building during working hours from 8:00 to 18:00 during weekdays. The residential EV will take a 25 km (2 h) ride to dinner outside every working day. It will also go for a 60 km trip every Sunday while staying in the residential building for the remaining period of weekends. Detailed schedules of each EV are illustrated in Fig. 3. The product of both two EVs is the "Tesla Model S" equipped with a 100 kWh-capacity lithium-ion battery supporting charging and discharging rates up to 1C [42]. The EV consumes 0.2 kWh per kilometer when cruising [43]. The latter Section 3.2.3 elaborates on the details of the EV control strategies.

The research is based on computer simulation using the advanced simulation software TRNSYS 18. TRNSYS is a renowned energy simulation software designed to model various types of energy systems,

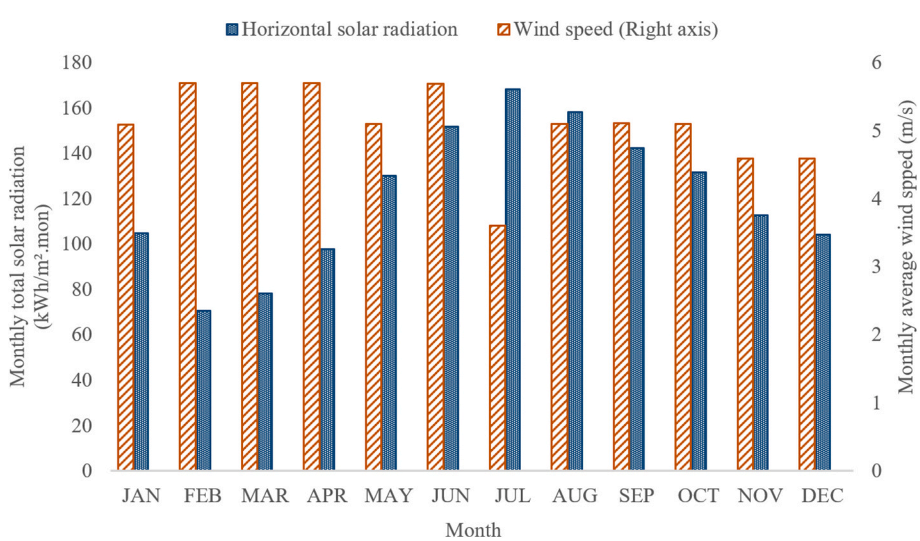

Fig. 1. The monthly horizontal total solar radiation and the monthly average wind speed in Hong Kong.

Table 1
The total energy and peak power demands of cooling, heating, and electric demands of the office building.

Office	Cooling			Heating				Electric
	AHU Cooling	Space Cooling	Total cooling	AHU Heating	Space Heating	DHW Heating	Total Heating	Electric (with Aux_tank)
Total Energy (kWh/m^2. a)	192.13	56.38	248.51	0.05	0.01	20.74	20.80	133.78
Peak Power (kW)	269.97	82·69	306.38	10.52	18.33	15.00	19.59	68.00

(a) Lighting, equipment, and ventilation fans except for the cooling and heating system and the electric vehicle system are included in the electric demand. (b) Reheating load by the cooling coil is not included in the AHU heating demand.

Table 2
The total energy and peak power demands of cooling, heating and electricity demands of the residential building.

Residence	Cooling			Heating				Electric
	AHU Cooling	Space Cooling	Total cooling	AHU Heating	Space Heating	DHW Heating	Total Heating	Electric (with Aux_tank)
Total Energy (kWh/m^2.a)	278.34	37.66	316.01	0.09	0.00	20.95	21.04	131.07
Peak Power (kW)	184.21	40.04	213.53	8.05	0.00	16.67	16.79	57.70

(a) Lighting, equipment, and ventilation fans except for the cooling and heating system and the electric vehicle system are included in the electric demand. (b) Reheating load by the cooling coil is not included in the AHU heating demand.

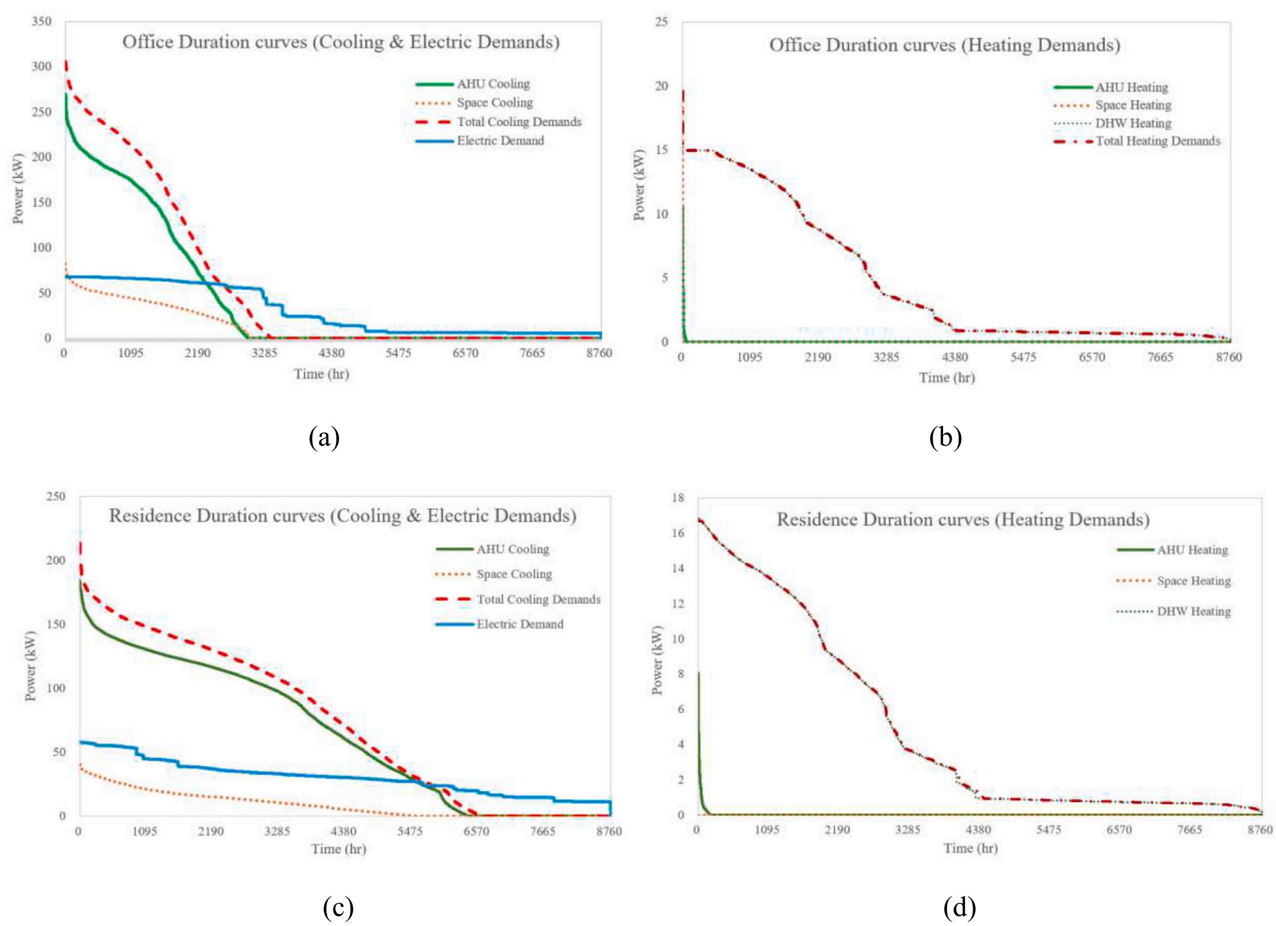

Fig. 2. The duration curves of cooling, heating, and electric demands of two buildings. (a) The duration curves of the office building of cooling and electric demand, (b) The duration curves of the office building of heating demand, (c) The duration curves of the residential building of cooling and electric demand, and (d) The duration curves of the residential building of heating demand.

including their consumption, as well as the generation and storage of renewable energy. This software utilizes the capabilities of the TRNSYS Simulation Studio, which is complemented by a built-in parametric analysis function and the energy simulation environment known as TRNBuild. Two buildings' hybrid energy systems integrated with micro-grid and two EVs are all configured with the TRNSYS 18 simulation environment. A parametric analysis is conducted first to analyze the impact of different renewable generation combinations. The impact of instantaneous and predictive micro-grid-based sharing and local EV-based sharing and their respective trading business model are further studied. Detailed methodology is described in Section 5. The time step of this study is set to 0.125 h to guarantee a stable and accurate simulation.

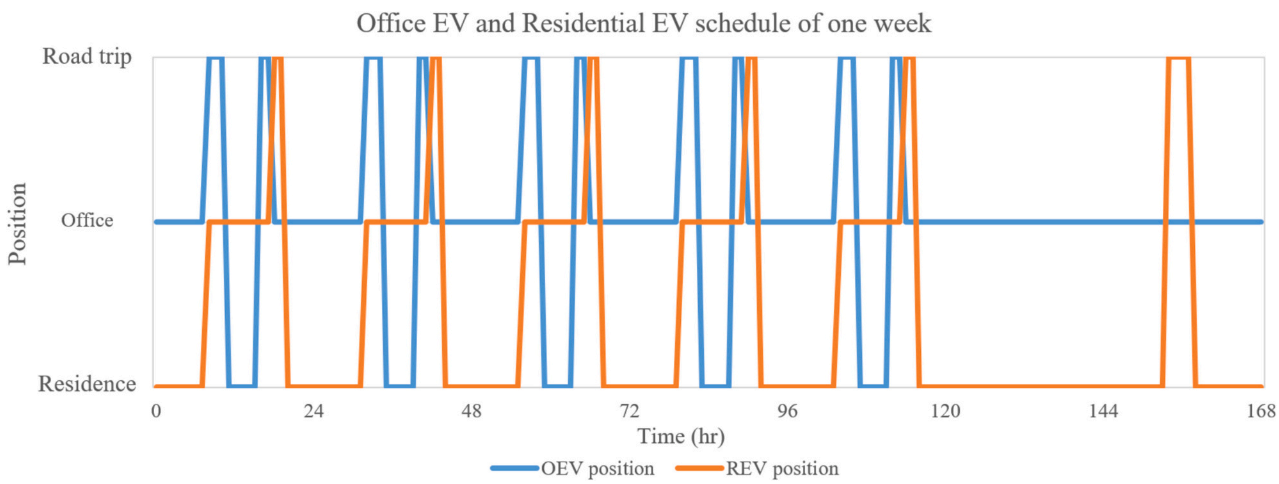

Fig. 3. The EV schedule of one week.

3. Building services systems

3.1. The primary elements and the system design principles

The primary elements of the compound system for two buildings consist of renewable energy generation systems, building energy consumption devices, and an integrated electric vehicle (EV) system, which are illustrated in Fig. 4. The renewables generation systems for both buildings include building-integrated photovoltaic systems (BIPV), floating photovoltaic systems (FPV), and onshore wind turbines, with specific details outlined in Section 3.3. The energy consumption devices within the buildings comprise water-cooled chillers (deployed in both the air-handling unit (AHU) cooling and space cooling systems), cooling towers, electric heaters for air and water, and other building operational equipment. The water-cooled chillers are responsible for charging the cooling storage tanks to meet the cooling requirements of the AHU and space cooling systems. Furthermore, each building's roof hosts a solar thermal hot water system supported by a hot water storage tank and an additional heater powered by electricity to fulfill the buildings' hot water demands. Due to each building's limited rooftop space, the area for solar thermal collectors is confined to 12 m^2, allocating the remainder for BIPV installations. In Table 3, the detailed information of the abovementioned components is given. For these two buildings, the EV integrated system consists of the building-to-vehicle (B2V) and

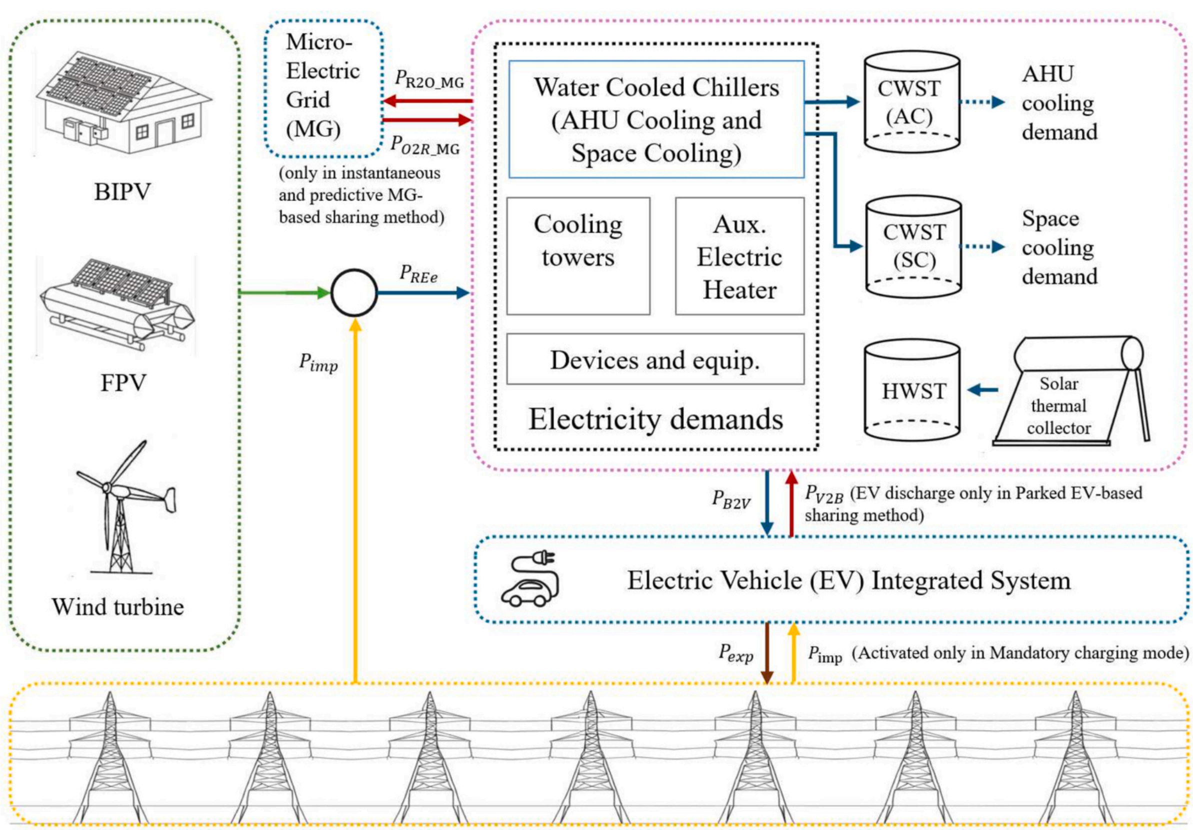

Fig. 4. The diagram of one grid-tied zero-energy building that incorporates the REe generation system, building service systems, and an integrated EV system. "CWST" and "HWST" refer to "cold water storage tank" and "hot water storage tank", respectively.

vehicle-to-building (V2B) functions. The two EVs can be charged via the B2V technologies of the EV-integrated system in all three energy sharing methods but can only be discharged via the V2B function in the local EV-based sharing mode.

Based on the general schematic shown in Fig. 4, three kinds of energy sharing methods, instantaneous and predictive micro-grid-based and local EV-based energy-sharing are novelly developed for each building. The performance of the three sharing methods will be discussed in the latter Section 5.2, 5.3 and 5.4. Both instantaneous micro-grid-based and local EV-based integrated energy-sharing methods are designed to encourage energy sharing between the two neighboring buildings. The control principles governing the buildings' hybrid system are slightly different due to the implementation of two different energy-sharing methods, which are outlined briefly as follows. On one hand, the control system initially assesses the amount of electricity produced by the renewable energy system and compares it to the electric demand of building devices and equipment. In instantaneous micro-grid-based sharing method, if the renewable electricity (REe) exceeds the need of own building electricity demand, the control system will divert the surplus electricity to the parked own EV charging. In the local EV-based sharing method, REe surplus after satisfying own building demands will be used to charge any local EV's battery. Thereafter, if the remaining surplus REe is still larger than zero, the remaining REe will be diverted to fulfill the demand of the neighboring building and its parked own EV by micro-grid in instantaneous micro-grid-based sharing method. In the local EV-based sharing scenario, the remaining REe will be transferred to the external grid. Alternatively, in case the REe cannot fully meet the electric demands of its building, the shortage gap will be covered by the micro-grid sharing first, then followed by importing electricity from the external grid if the micro-grid sharing amount is still not sufficient. For EV sharing, the local EV will discharge its battery to meet the electricity shortage in case REe is not enough if the condition allows. The building will import electricity from the electric grid if the discharging still cannot fill the gap. As for the predictive micro-grid-based energy sharing method, it has nothing different from the instantaneous micro-grid-based energy sharing except that is based on the presumption that the future energy generation and demand information of the residential building is already known beforehand. The execution of micro-grid sharing is determined by the future energy condition and trading price to maximize one of the stakeholder's economic interests. The detailed expatriation of these three energy-sharing control strategies is described in the latter Section 3.2.

Table 3
The setting index of chillers and solar thermal collectors in TRNSYS settings.

	The contents	The parameters
AHU and Space Cooling Chillers (Modelled by the Type 666 [44] in the TRNSYS	Chiller type	AHU cooling chiller: Water-cooled chiller. Product parameters are based on "Daikin WGZ090"(office), "Daikin WGZ060"(residence)
		Space cooling chiller: Water-cooled chiller. Product parameters are based on "Daikin WGZ030"(office and residence)
	Rated capacity[(a)]	AHU cooling chiller: 307.7 kW (office), 213.7 kW (residence)
		Space cooling chiller: 106.0 kW (office and residence)
	Rated COP[(a)]	AHU cooling chiller: 4.6 (office), 4.5 (residence)
		Space cooling chiller: 4.5 (office and residence)
	Set point temperature of the chilled water leaving temperature	AHU cooling chiller: 5 °C (office and residence)
		Space cooling chiller: 13 °C (office and residence)
Solar Thermal Collectors (Modelled by the Type 71 [44] in TRNSYS	Type	Evacuated tube solar thermal collector
	The dimensions of solar thermal systems	12 modules with each module at $1m^2$
	Number in serious times the number in parallel	3×4
	Flow rate at test conditions	50 kg/(hr. m^2)
	Intercept efficiency	0.7
	Negative of first order efficiency coefficient	2.78 W/(m^2.K^2)
	Negative of second order efficiency coefficient	8.33

(a) The rated condition includes an inlet cooling water temperature of 35 °C and a chilled water set point temperature of 7 °C.

3.2. The elaborated control strategies for energy-sharing between the two neighboring buildings

3.2.1. The instantaneous micro-grid-based energy-sharing method

In instantaneous micro-grid-based energy-sharing method, the only energy sharing method between two neighboring buildings is by micro-grid. In order to study the influence of micro-grid sharing, there is no V2B function in this sharing mode. Under the instantaneous micro-grid-based energy-sharing method, the energy management system makes all decisions of sharing energy by micro-grid based on current energy condition of both buildings surplus or shortage. As the abovementioned control principles of instantaneous micro-grid sharing illustrate, the generated renewable electricity (REe) of each building will be firstly used to fulfill the demand of its own building. When there is still remaining surplus energy available, it will charge the parked own EV. In case the own EV is not parked in its own building or the surplus REe exceeds the maximum charging power 1C of the EV battery, the remaining electricity will be transferred to the neighboring building by micro-grid sharing if it is in energy shortage. Thereafter, after meeting the demand for its own building along with its own EV and the shortage of the neighboring building, if there is still a surplus left, the remaining REe will charge the parked neighboring building's EV. In the following three scenarios that the REe of the neighboring building can fully support its own demands, or another stakeholder's EV is not parked in its own building, or the left surplus REe is beyond the maximum charging power of the EV, the left surplus energy will be exported to the external grid. On the contrary, when the REe generation fails to cover its own building's demands, the control strategy will consider transferring energy through micro-grid sharing from the neighboring building. If the amount of micro-grid transferred electricity is not sufficient or the neighboring building itself is in shortage, importing electricity from the external grid will be the final option. Detailed control strategies logic and general mathematics formula are presented in Fig. 5 and Table 4.

3.2.2. The predictive micro-grid-based energy-sharing method

The predictive micro-grid-based energy-sharing method is developed based on the instantaneous micro-grid-based energy-sharing method. Unlike instantaneous energy-sharing control that encourages energy sharing between two buildings, predictive energy-sharing control make sharing decisions in the line with one of the stakeholder's economic benefits instead of sharing whenever possible. This sharing method is called "predictive" because that the decision is made based on the information of building's future energy generation and demand that is presumed already known beforehand. The decision of sharing is based on the Decision-Making Index (DMI) that is determined by two variables, the future energy situation and the trading price value, which details will be explained in the latter paragraph. There are 52 out of 81 cases in the residential building transfers more micro-grid sharing than the office building in instantaneous micro-grid sharing, therefore in this model the residential building is selected as the studied object about

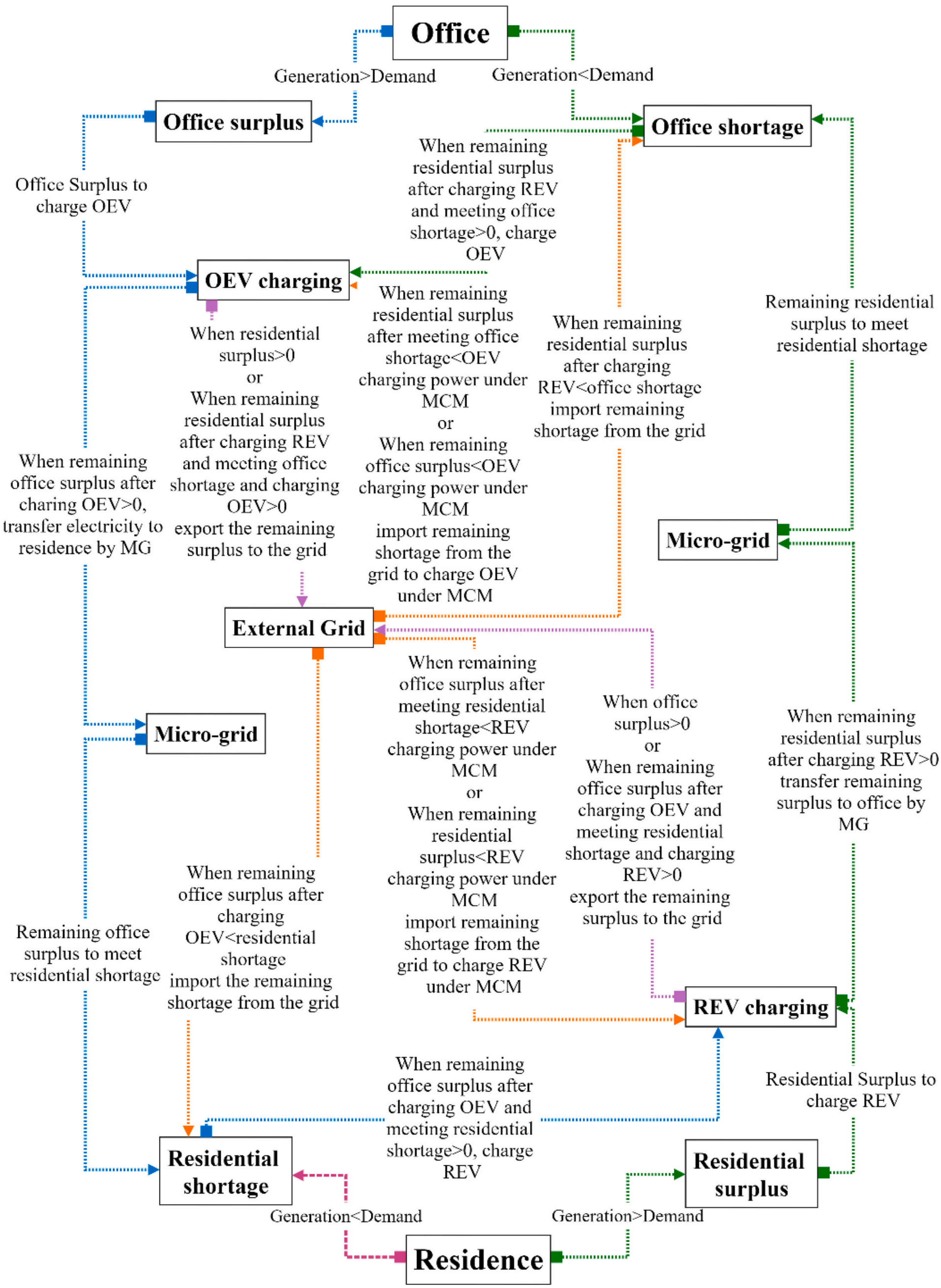

Fig. 5. The instantaneous micro-grid-based energy-sharing control strategy chart. "MCM" refers to "Mandatory charging mode" as introduced in Section 3.2.3.

how these two variables will affect the building systems' efficacy in technical and economic aspects. An additional 100 kWh building battery is installed in the residential building as energy storage to provide flexibility for the energy control system to reduce micro-grid sharing amount and the trading fee. If the trading price is high, or the control system predicts there will be much surplus energy in the coming future

Table 4
Modelling formulation of renewable generation system, EV and grid interactions under instantaneous micro-grid-based energy-sharing method.

Equation	Explanation
$\int_0^{8760h} Gen_{OffRe}(t)dt = \int_0^{8760h} [Gen_{OffBIPV}(t) + Gen_{OffFPV}(t) + Gen_{OffWT}(t)]dt$ $\int_0^{8760h} Gen_{ResRe}(t)dt = \int_0^{8760h} [Gen_{ResBIPV}(t) + Gen_{ResFPV}(t) + Gen_{ResWT}(t)]dt$	Generation of renewable energy of each building
$\int_0^{8760h} Gap_{Off}(t)dt = \int_0^{8760h} [Gen_{OffRe}(t) - Demand_{Off}(t)]dt$ $\int_0^{8760h} Gap_{Res}(t)dt = \int_0^{8760h} [Gen_{ResRe}(t) - Demand_{Res}(t)]dt$	Energy gap between the generation and the demand of each building
$\int_0^{8760h} CH_{OEV}(t)dt = \int_0^{8760h} If(FSOC_{OEV} < 0.95, 1, 0) \times \begin{cases} If[Gap_{Off}(t) \geq 0, Gap_{Off}(t), 0]dt \\ If\{Gap_{Off}(t) < 0, If[Gap_{Res}(t) - CH_{REV}(t) - \lvert Gap_{Off}(t) \rvert \geq 0, Gap_{Res}(t) - CH_{REV}(t) - \lvert Gap_{Off}(t) \rvert, 0], 0\}dt \end{cases}$ $\int_0^{8760h} CH_{REV}(t)dt = \int_0^{8760h} If(FSOC_{REV} < 0.95, 1, 0) \times \begin{cases} If[Gap_{Res}(t) \geq 0, Gap_{Res}(t), 0]dt \\ If\{Gap_{Res}(t) < 0, If[Gap_{Off}(t) - CH_{OEV}(t) - \lvert Gap_{Res}(t) \rvert \geq 0, Gap_{Off}(t) - CH_{OEV}(t) - \lvert Gap_{Res}(t) \rvert, 0], 0\}dt \end{cases}$	Each EV Charging energy amount
$\int_0^{8760h} MG_{O2R}(t)dt = \int_0^{8760h} \{If[Gap_{Off}(t) - CH_{OEV}(t) > 0, 1, 0] \times If[Gap_{Res}(t) < 0, 1, 0] \times [Gap_{Off}(t) - CH_{OEV}(t)]\}dt$ $\int_0^{8760h} MG_{R2O}(t)dt = \int_0^{8760h} \{If[Gap_{Res}(t) - CH_{REV}(t) > 0, 1, 0] \times If[Gap_{Off}(t) < 0, 1, 0] \times [Gap_{Res}(t) - CH_{REV}(t)]\}dt$	Energy sharing amount by micro-grid of two directions
$\int_0^{8760h} E_{Offimp.a}(t)dt = \int_0^{8760h} [Demand_{Off}(t) - Gen_{OffRe}(t) - MG_{R2O}(t)]dt$ $\int_0^{8760h} E_{Resimp.a}(t)dt = \int_0^{8760h} [Demand_{Res}(t) - Gen_{ResRe}(t) - MG_{O2R}(t)]dt$	Energy import from power grid of each building
$\int_0^{8760h} E_{Offexp.a}(t)dt = \int_0^{8760h} [Gen_{OffRe}(t) - Demand_{Off}(t) - CH_{OEV}(t) - MG_{O2R}(t)]dt$ $\int_0^{8760h} E_{Resexp.a}(t)dt = \int_0^{8760h} [Gen_{ResRe}(t) - Demand_{RES}(t) - CH_{REV}(t) - MG_{R2O}(t)]dt$	Energy export to power grid of each building

based on the existing annual data of renewable generation and building demand, or a combination of both, it tends to use the battery storage energy instead of micro-grid sharing energy to avoid paying unnecessary trading fee. On the contrary, if the trading price is low, or the building is anticipated to face significant shortages in the future, or both, the control system will prioritize the utilization of micro-grid sharing initially, reserving the stored energy in the battery for impending shortages to save money from importing electricity from the external grid.

$$DMI_R = 0.5 \bullet FactorTP + 0.5 \bullet FactorFE \tag{1}$$

$$FactorTP = -0.64935 \bullet TP + 1 \tag{2}$$

$$FactorFE = \frac{1}{min\left\{\sum_{i=step}^{step+192} GAP_i \mid step \in [0, 69888]\right\} - max\left\{\sum_{i=step}^{step+192} GAP_i \mid step \in [0, 69888]\right\}} \bullet \sum_{i=step}^{step+192} GAP_i + \frac{max\left\{\sum_{i=step}^{step+192} GAP_i \mid step \in [0, 69888]\right\}}{max\left\{\sum_{i=step}^{step+192} GAP_i \mid step \in [0, 69888]\right\} - min\left\{\sum_{i=step}^{step+192} GAP_i \mid step \in [0, 69888]\right\}} \tag{3}$$

$$GAP_{step} = GENERATION_{step} - DEMAND_{step} \tag{4}$$

In this scenario, the Decision-Making Index of residential building (DMI_R) is introduced to evaluate whether to use spare energy by micro-grid from another building based on the own building future situation (next 24 h) and the trading price. When DMI_R is larger or equal to 0.5, the residential building use the energy from the office building by micro-grid if the following two conditions are met: 1) the residential building has energy shortages; 2) the office building has an energy surplus. Otherwise, the system uses the residential battery to satisfy the building shortages. *FactorTP* determines the impact of trading price change. When the price equals to 0, then *FactorTP* equals to 1, DMI_R is equal or larger than 0.5, which means the micro-grid sharing will be conducted as much as possible. When the trading price is close to the external power grid price, it will result in a lower *FactorTP*, hence lower chance for DMI_R higher than 0.5. *FactorFE* refers to the future 24-h energy situation. Based on the existing data of building renewable generation and demand, $\sum_{i=step}^{step+192} GAP_{step}$ means the sum-up value of energy surplus (positive) or shortages (negative) for the next 192 time step (each step equals to 0.125 h, 192 steps equal to 24 h) at the current time step, while $min\left\{\sum_{i=step}^{step+192} GAP_{step} \mid step \in [0, 69888]\right\}$ and $max\left\{\sum_{i=step}^{step+192} GAP_{step} \mid step \in [0, 69888]\right\}$ represents the minimum and the maximum accumulated sum-up values of the considered future time period (24 h) in one year (total 70,080 steps), respectively. When the sum-up value of the next 24 h energy is progressively closer to the maximum annual accumulated sum-up value then *FactorFE* will be increasingly closer to 0, it indicates that the building is more likely to possess much surplus in the coming 24 h, therefore the decision is made that it is not necessary to receive micro-grid sharing electricity at this current time step. The logic is opposite when the 24-h sum-up value is approximate to the minimum annual accumulated sum-up value, causing higher possibilities to use transferred electricity from micro-grid. There are two differences between the instantaneous micro-grid-based control strategy mentioned in Section 3.2.1 and the predictive micro-grid-based control strategy. One of the differences is that when the conditions are allowed to conduct micro-grid sharing from office to residential building under instantaneous micro-grid-based sharing, the predictive micro-grid-based control will judge whether the DMI_R is larger than 0.5. If the DMI_R is lower than 0.5, which the future 24-h energy surplus is likely to be sufficient enough to meet the demand or the trading price is high or a combination of both, the residence will decline to accept office surplus through micro-grid to avoid paying unnecessary trading fee, therefore the office surplus will be exported to the external grid. Another difference is adding one building battery in the residential building to provide control flexibility. As long as the residential building has surplus energy, the residential battery will have the top priority to be

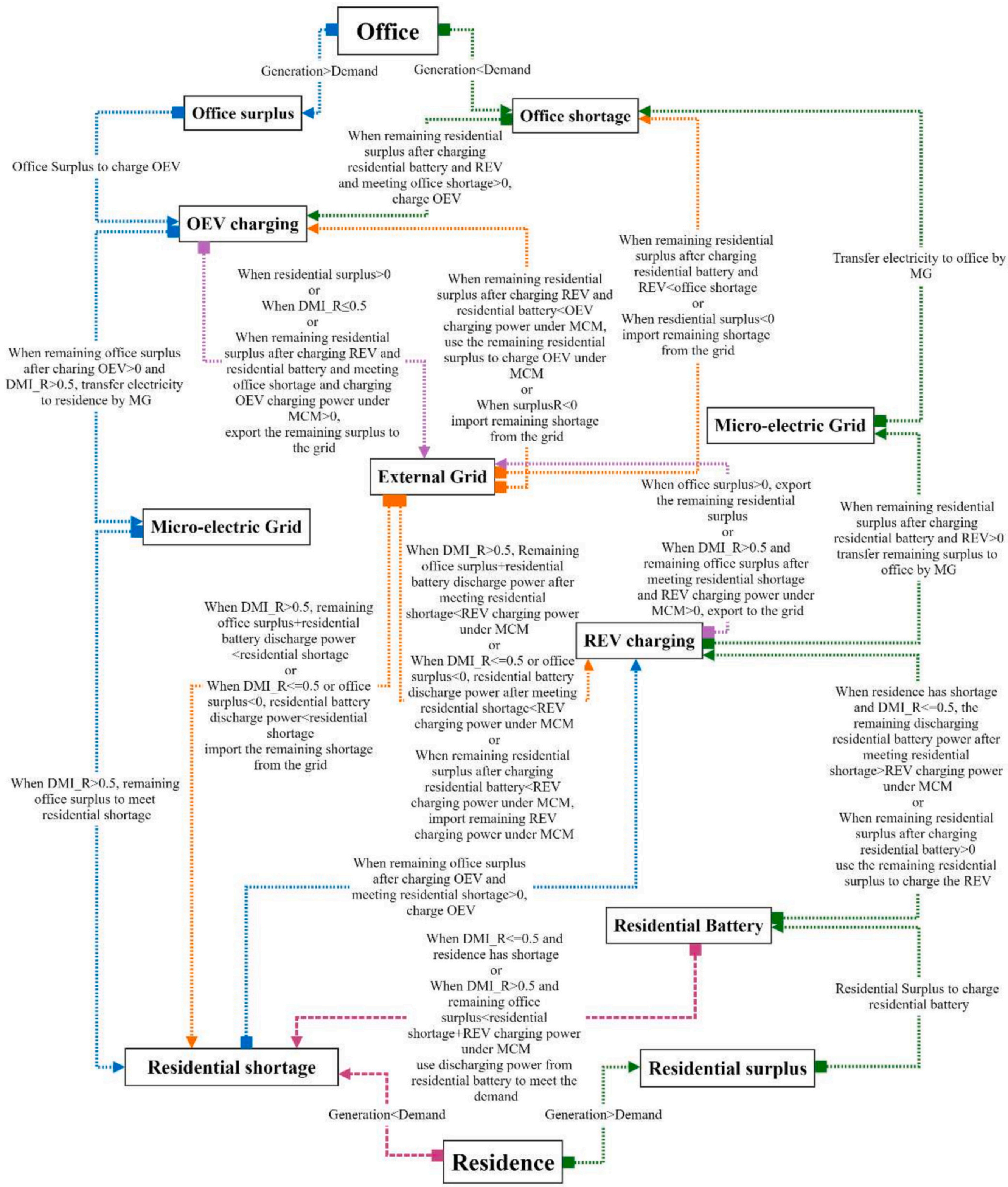

Fig. 6. The perfect predictive Micro-grid control strategy. "MCM" refers to "Mandatory charging mode" as introduced in Section 3.2.3.

charged, followed by the residential EV. When encountering residential shortages, DMI_R falls below 0.5 and no office surplus, the residential battery will discharge to address the shortages. Any remaining deficit will be compensated by importing energy from the power grid. The detailed predictive micro-grid-based control strategy and the mathematic formula of energy flow for the DMI_R-applied management system are shown in Fig. 6 and Table 5, respectively.

The results of another control strategy called the instantaneous micro-grid-based sharing with residential battery are also added in Section 5.3. The design of this control strategy is nothing different from the predictive micro-grid-based sharing control except that there is no DMI control on the micro-grid sharing, so that the differences of

Table 5
Modelling formulation of renewable generation system, EV and grid interactions under predictive micro-grid-based energy-sharing method.

Equation	Explanation
$\int_0^{8760h} Gen_{OffRe}(t)dt = \int_0^{8760h} \left[Gen_{OffBIPV}(t) + Gen_{OffFPV}(t) + Gen_{OffWT}(t)\right]dt$	Generation of renewable energy of each building
$\int_0^{8760h} Gen_{ResRe}(t)dt = \int_0^{8760h} [Gen_{ResBIPV}(t) + Gen_{ResFPV}(t) + Gen_{ResWT}(t)]dt$	
$\int_0^{8760h} Gap_{Off}(t)dt = \int_0^{8760h} \left[Gen_{OffRe}(t) - Demand_{Off}(t)\right]dt$	Energy gap between the generation and the demand of each building
$\int_0^{8760h} Gap_{Res}(t)dt = \int_0^{8760h} [Gen_{ResRe}(t) - Demand_{Res}(t)]dt$	
$\int_0^{8760h} CH_{OEV}(t)dt = \int_0^{8760h} If(FSOC_{OEV} < 0.95, 1, 0) \times \left\{ \begin{array}{c} If\left[Gap_{Off}(t) \geq 0, Gap_{Off}(t), 0\right]dt \\ If\left\{Gap_{Off}(t) < 0, If\left[Gap_{Res}(t) - CH_{RB}(t) - CH_{REV}(t) - \left\lvert Gap_{Off}(t)\right\rvert \geq 0, Gap_{Res}(t) - CH_{RB}(t) - CH_{REV}(t) - \left\lvert Gap_{Off}(t)\right\rvert, 0\right], 0\right\}dt \end{array} \right.$	Each EV Charging energy amount
$\int_0^{8760h} CH_{REV}(t)dt = \int_0^{8760h} If(FSOC_{REV} < 0.95, 1, 0) \times \left\{ \begin{array}{c} If[Gap_{Res}(t) - CH_{RB}(t) \geq 0, Gap_{Res}(t), 0]dt \\ If\left\{Gap_{Res}(t) < 0, If\left[Gap_{Off}(t) - CH_{OEV}(t) - \lvert Gap_{Res}(t)\rvert \geq 0, Gap_{Off}(t) - CH_{OEV}(t) - \lvert Gap_{Res}(t)\rvert, 0\right], 0\right\}dt \end{array} \right.$	
$\int_0^{8760h} CH_{RB}(t)dt = \int_0^{8760h} \{If(FSOC_{RB} < 0.95, 1, 0) \times If[Gap_{Res}(t) \geq 0, Gap_{Res}(t), 0]\}dt$	
$\int_0^{8760h} MG_{O2R}(t)dt = \int_0^{8760h} \left\{If\left[Gap_{Off}(t) - CH_{OEV}(t) > 0, 1, 0\right] \times If[Gap_{Res}(t) < 0, 1, 0] \times If[DMI_R > 0.5, 1, 0] \times \left[Gap_{Off}(t) - CH_{OEV}(t)\right]\right\}dt$	Energy sharing amount by micro-grid of two directions
$\int_0^{8760h} MG_{R2O}(t)dt = \int_0^{8760h} \left\{If[Gap_{Res}(t) - CH_{RB}(t) - CH_{REV}(t) > 0, 1, 0] \times If\left[Gap_{Off}(t) < 0, 1, 0\right] \times [Gap_{Res}(t) - CH_{RB}(t) - CH_{REV}(t)]\right\}dt$	
$\int_0^{8760h} E_{Offimp.a}(t)dt = \int_0^{8760h} \left[Demand_{Off}(t) - Gen_{OffRe}(t) - MG_{R2O}(t)\right]dt$	Energy import from power grid of each building
$\int_0^{8760h} E_{Resimp.a}(t)dt = \int_0^{8760h} [Demand_{Res}(t) - Gen_{ResRe}(t) - MG_{O2R}(t)]dt$	
$\int_0^{8760h} E_{Offexp.a}(t)dt = \int_0^{8760h} \left[Gen_{OffRe}(t) - Demand_{Off}(t) - CH_{OEV}(t) - MG_{O2R}(t)\right]dt$	Energy export to power grid of each building
$\int_0^{8760h} E_{Resexp.a}(t)dt = \int_0^{8760h} [Gen_{ResRe}(t) - Demand_{RES}(t) - CH_{RB}(t) - CH_{REV}(t) - MG_{R2O}(t)]dt$	

predictive control can be compared based on the same reference line. In other words, this control strategy is an enhanced version of the instantaneous micro-grid-based energy-sharing described in Section 3.2.1.

3.2.3. The local electric-vehicle-based energy-sharing method

In local EV-based sharing mode, two neighboring buildings share electricity through their two EVs' charging and discharging functions at different locations according to the schedule. There is no electricity sharing by any physical cables so the sole impact of EV sharing can be studied. Similar to the instantaneous micro-grid-based energy-sharing, the management system makes decision of whether charging or discharging EV solely based on current energy condition of the building. As mentioned in Section 3.1, the REe will cover its own building demand first similar to the micro-grid-based sharing method. If REe generation is more than the need of own building, the remaining REe will be diverted to charge the local EV if the conditions allow. In cases where there is no EV parked in the building or the remaining surplus REe power exceeds the maximum charging power, the unused electricity will be sent to the external power grid. Inversely, if the own building needs more energy than the renewable system can provide, the system will discharge the local EV first if its FSOC level allows it. Otherwise, the deficit in building energy will be addressed through the importation of electricity from the external grid. The detailed control logic and equation formula are illustrated in Fig. 7 and Table 6, respectively.

(1) The control strategy of the B2V process in three integrated energy-sharing methods

As stated in Section 2, the EV model employed in this research is the "Tesla Model S," which has a battery capacity of 100 kWh. Type 47a in TRNSYS software is a powerful model to simulate this battery [44]. The fractional state of charge (FSOC) is used in this model to indicate the available percentage of storage electricity in each battery. The maximum charging limit for each EV battery is set to FSOC 0.95 and the minimum of FSOC 0.30 to protect the lithium battery. Furthermore, the FSOC for both the office EV and the residential EV should not be less than 0.30 after the trips finish. Therefore, both EVs' battery FSOC are monitored at certain hours before the departure time depending on the coming trip length. In case the FSOC at departure time is less than the minimum required level to guarantee the FSOC is not lower than 0.30 when the trip ends, a "mandatory charging mode (MCM)" is activated with a minimum charging power that ensures the EV battery can be increased to the required FSOC for the upcoming trip. The minimum charging power in this mode is preferentially supported by the renewable generation REe; when this surplus REe is less than the required power, the rest gap will be filled by importation from the external grid. Once the FSOC reaches the minimum required level for the incoming trip, the "mandatory charging mode" is deactivated while the "normal charging mode" kicks in. The "normal charging mode" is executed if the conditions mentioned below are all met: (a) The own building's renewable generation exceeds its building demand in all sharing modes or the condition of energy-sharing by micro-grid allows in two micro-grid-based sharing mode; (b) The EV is parked in any building in EV-based sharing mode or in its own building in micro-grid-based sharing mode; (c) The EV battery FSOC has not reached the upper limit 0.95.

(2) The control strategy of the V2B process

The EV battery discharges only in the local EV-based energy-sharing mode. Discharging occurs when three following conditions are met: (a) There is a shortage in the building's electricity supply; (b) The EV is parked in the building; (c) The EV battery's FSOC is above the minimum required level for the next planned trip.

3.3. The renewable electricity generation systems

In previous Section 3.1, the renewable electricity generation system is described as consisting of three components: building-integrated photovoltaic system (BIPV), floating photovoltaic system (FPV), and wind turbine system. The specific features of these systems are described below.

3.3.1. The system design of solar energy

(1) Building-Integrated Photovoltaics (BIPV)

Solar energy is one of the most effective renewables resources in cities. Considering Hong Kong is a highly building-intensive city with

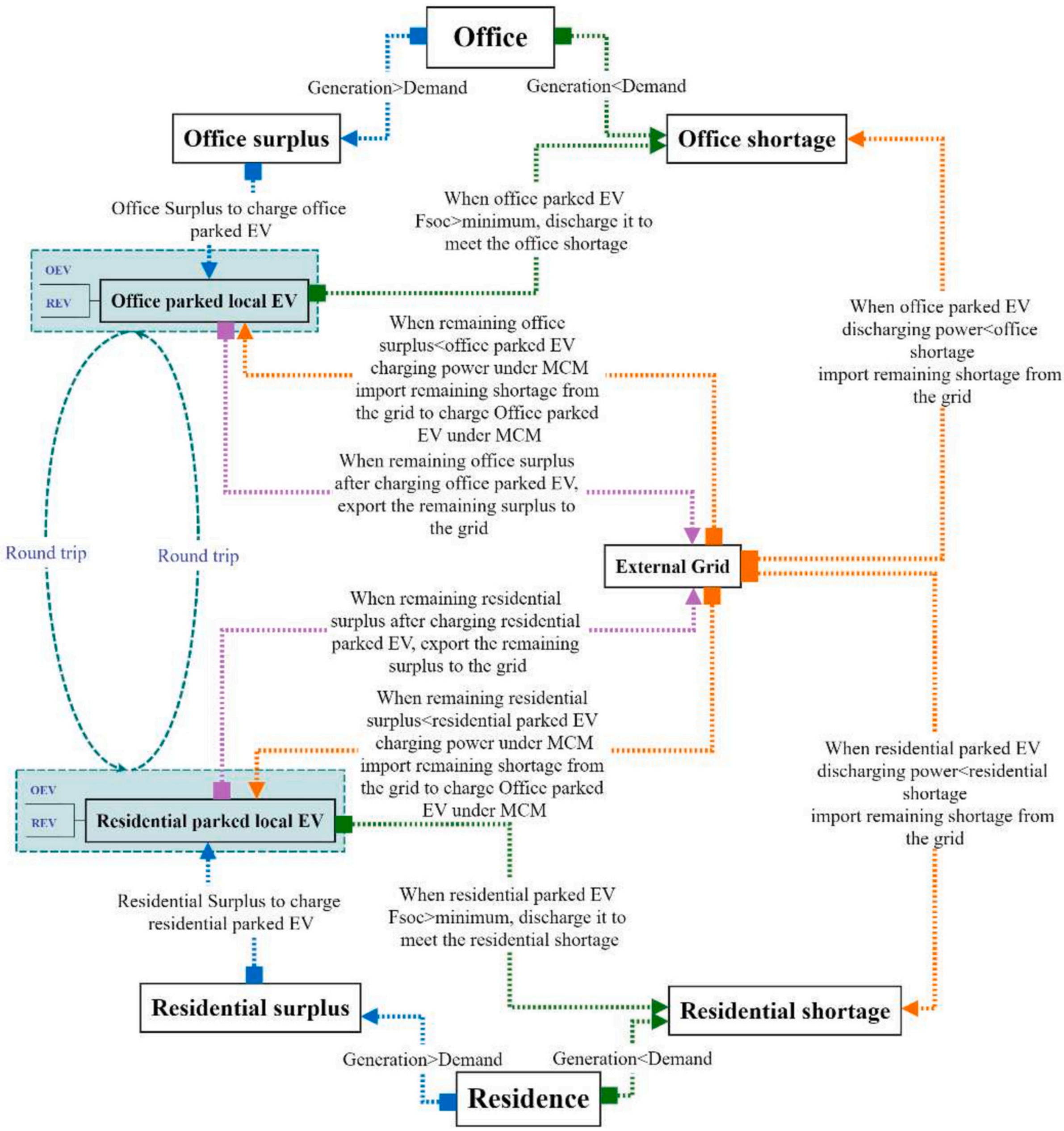

Fig. 7. The Local EV-based energy-sharing control strategy chart. "MCM" refers to "Mandatory charging mode" as introduced in Section 3.2.3.

little spare space, it is advisable to make use of the flat roof surface to install BIPVs. In both office and residential buildings, if the renewable energy system includes BIPV, these are installed on flat roofs, covering 86.6 % (346.44 m^2) of the roof area. The remaining space is occupied by solar thermal collectors and other roof-mounted devices. The surface of BIPV is made of a glazing panel with an air gap between the panel and the roof structure. The BIPV, which is a commercial product "FU 275 P" manufactured by the FuturaSun Company [45], is modelled by the TRNSYS Type190 [44] which employs a five-parameter circuit model. This polycrystalline photovoltaic module can achieve 16.84 % efficiency under the standard test condition (STC: 1000 W/m^2, reference temperature 25 °C) based on the product handbook [45]. Further details about this BIPV product can be found in Table 7.

(2) Floating photovoltaics (FPV)

Given the limited roof surface area, the efficiency of existing solar energy technologies is insufficient to satisfy building energy demands. The need for land resources to install photovoltaics (PV) is contradictory to the highly developed urbanization and population density in Hong Kong. Hence, since the two buildings are both located on the shore, it is reasonable to utilize the sea surface near the target buildings in case the renewables system of each building is comprised of FPVs. Moreover, the FPV panels are positioned horizontally to the calm sea surface to minimize orientation changes caused by wind and waves. The selected commercial product for FPV is also "FU 275 P" [45]and it is modelled in TRNSYS by Type 567 [46] since it considers the impact of seawater temperature on FPV generation efficiency, which can show the advantages of FPV systems [47,48]. The detailed parameters of this product under STC are shown in Table 7.

3.3.2. *The system design of wind energy*

The two buildings are located on the seashore, where there is plenty of wind energy created by the land-ocean temperature difference and the subtropical monsoon. So, the wind turbines are assumed to be locally installed on the nearby seashore of these buildings. The selected on-

Table 6
Modelling formulation of renewable generation system, EV and grid interactions under local EV-based energy-sharing method. "$OEV_{location}$" means the location of office EV, which the value "1" means the office EV is parked in the office and the value "0" means the office EV is parked in the residence. "$REV_{location}$" means the location of residential EV, which the value "0" means the residential EV is parked in the residence and the value "1" means the residential EV is parked in the office.

Equation	Explanation
$\int_0^{8760h} Gen_{OffRe}(t)dt = \int_0^{8760h} \left[Gen_{OffBIPV}(t) + Gen_{OffFPV}(t) + Gen_{OffWT}(t)\right]dt$ $\int_0^{8760h} Gen_{ResRe}(t)dt = \int_0^{8760h} \left[Gen_{ResBIPV}(t) + Gen_{ResFPV}(t) + Gen_{ResWT}(t)\right]dt$	Generation of renewable energy of each building
$\int_0^{8760h} Gap_{Off}(t)dt = \int_0^{8760h} \left[Gen_{OffRe}(t) - Demand_{Off}(t)\right]dt$ $\int_0^{8760h} Gap_{Res}(t)dt = \int_0^{8760h} \left[Gen_{ResRe}(t) - Demand_{Res}(t)\right]dt$	Energy gap between the generation and the demand of each building
$\int_0^{8760h} CH_{OEV}(t)dt = \int_0^{8760h} If(FSOC_{OEV} < 0.95, 1, 0) \times \begin{cases} If[OEV_{location} = 1, 1, 0] \times If\left[Gap_{Off}(t) \geq 0, Gap_{Off}(t), 0\right]dt \\ If[OEV_{location} = 0, 1, 0] \times If[Gap_{Res}(t) \geq 0, Gap_{Res}(t), 0]dt \end{cases}$ $\int_0^{8760h} CH_{REV}(t)dt = \int_0^{8760h} If(FSOC_{REV} < 0.95, 1, 0) \times \begin{cases} If[REV_{location} = 0, 1, 0] \times If[Gap_{Res}(t) \geq 0, Gap_{Res}(t), 0]dt \\ If[REV_{location} = 1, 1, 0] \times If\left[Gap_{Off}(t) \geq 0, Gap_{Off}(t), 0\right]dt \end{cases}$	Each EV Charging energy amount
$\int_0^{8760h} DisCH_{OEV}(t)dt = \int_0^{8760h} If(FSOC_{OEV} > 0.3, 1, 0) \times \begin{cases} If[OEV_{location} = 1, 1, 0] \times If\left[Gap_{Off}(t) < 0, \left\|Gap_{Off}(t)\right\|, 0\right]dt \\ If[OEV_{location} = 0, 1, 0] \times If[Gap_{Res}(t) < 0, \|Gap_{Res}(t)\|, 0]dt \end{cases}$ $\int_0^{8760h} DisCH_{REV}(t)dt = \int_0^{8760h} If(FSOC_{REV} > 0.3, 1, 0) \times \begin{cases} If[REV_{location} = 0, 1, 0] \times If[Gap_{Res}(t) < 0, \|Gap_{Res}(t)\|, 0]dt \\ If[REV_{location} = 1, 1, 0] \times If\left[Gap_{Off}(t) < 0, \left\|Gap_{Off}(t)\right\|, 0\right]dt \end{cases}$	Each EV Discharging energy amount
$\int_0^{8760h} E_{Offimp.a}(t)dt = \int_0^{8760h} \left[Demand_{Off}(t) - Gen_{OffRe}(t) - DisCH_{OEV}(t) - DisCH_{REV}(t)\right]dt$ $\int_0^{8760h} E_{Resimp.a}(t)dt = \int_0^{8760h} \left[Demand_{Res}(t) - Gen_{ResRe}(t) - DisCH_{REV}(t) - DisCH_{OEV}(t)\right]dt$	Energy import from power grid of each building
$\int_0^{8760h} E_{Offexp.a}(t)dt = \int_0^{8760h} \left[Gen_{OffRe}(t) - Demand_{Off}(t) - CH_{OEV}(t)\right]dt$ $\int_0^{8760h} E_{Resexp.a}(t)dt = \int_0^{8760h} \left[Gen_{ResRe}(t) - Demand_{RES}(t) - CH_{REV}(t)\right]dt$	Energy export to power grid of each building

shore small-scale wind turbine product for these two buildings is "ET-WT10KL-W [49]" with a rated power of 10 kW each. It features a horizontal-axis design with three blades, a hub height of 22 m, and a rotor diameter of 7 m. The working wind speed is from 3 to 30 m/s. The wind turbine is simulated using the Type 90 model in TRNSYS [44] This model calculates power generation primarily using a power-wind speed curve, while also considering factors such as control mode, hub height, land roughness and air properties. The number of wind turbines is one of the parameters studied in subsequent parametric analyses. Table 7 delineates the comprehensive index of the product as specified by the manufacturer.

4. Analysis criteria

Multiple technical and economic analysis criteria are employed to assess the results and compare the enhancements in techno-economic performance investigated in this research. This section outlines the definitions and equations associated with these analysis criteria.

Firstly, the concepts of on-site electrical energy faction (*OEFe*) and electrical energy matching (*OEMe*) are introduced to evaluate the matching capability between building systems and external electric grid. *OEFe* is the indicator that shows the proportion of own building demand satisfied by the local renewable energy generation without importing from the grid. *OEMe* is the indicator that quantifies the percentage of locally generated renewable energy that is utilized to meet the building's own energy requirements. The WMI is the average value of *OEFe* and *OEMe* that indicates the comprehensive matching capability between building and the grid. The simplified format of the *OEFe*, *OEMe*

Table 7
The index of BIPV, FPV and wind turbine in TRNSYS settings.

	The contents	The parameters
BIPV	Type model	5 parameters equivalent circuit model
	MPPT mode	The PV is equipped with a maximum power point tracking (MPPT) device
	Module short-circuit current at reference conditions	9.11 A
	Module open-circuit voltage at reference conditions	38.65 V
	Reference cell temperature	298 K
	Reference insolation	1000 W/m^2
	Module current at max power point and reference conditions	8.73 A
	Module voltage at max power point and reference conditions	31.52 V
	Temperature coefficient of Isc (ref. cond)	0.0474 %
	Temperature coefficient of Voc (ref. cond)	−0.285 V/K
	Module temperature at NOCT	313 K
	Ambient temperature at NOCT	293 K
	Insolation at NOCT	800 W/m^2
	Module area	1.474 m^2
	The product of the module cover's transmittance and the substrate's absorptance for solar radiation normal to the plane of the module.	0.95
	Semiconductor bandgap	1.12 eV
	Value of parameter "a" at reference conditions	1.976
	Value of parameter I_L at reference conditions	5.417 A
	Value of parameter I_0 at reference conditions	1.104×10^{-9}
	Module series resistance	0.5195 Ω
	Shunt resistance at reference conditions	161 Ω
Floating PV	PV efficiency mode	Linear modifiers for off-rated cell temperature and incident radiation
	The PV surface absorptance	0.9
	Product dimensions	1650 × 990 × 35 mm
	The transparent cover material refractive index	1.526
	The reference PV efficiency under the reference conditions (the incidence radiation at 1000 W/m2 and the reference temperature at 25 °C)	16.84 %
	Efficiency modifier regarding to the temperature	−0.0037/C
	Efficiency modifier regarding to the radiation	m^2/W
	The glazing cover surface emissivity	0.9
	The glazing cover conductivity	0.8 W/(m.K)
	The glazing cover thickness	0.0032 m
Wind turbine	The type of the wind turbine	3-blade horizontal-axis wind turbine (based on the commercial product "ET-WT10KL-W [49]")
	Rated power	10 kW
	Hub height	22 m
	Rotor diameter	7 m
	Cut-in wind speed	3 m/s
	Cut-out wind speed	30 m/s
	The site shear exponent	0.1

and *WMI* are as follows, while the detailed calculation methods are defined in the Ref. [50,51]:

$$OEFe = 1 - \frac{\int_{t1}^{t2} P_{imp}(t)dt}{\int_{t1}^{t2} [L_{elec}(t) + P_{B2V}(t)]dt}, 0 \leq OEFe \leq 1 \tag{5}$$

$$OEMe = 1 - \frac{\int_{t1}^{t2} P_{exp}(t)dt}{\int_{t1}^{t2} P_{REe}(t)dt}, 0 \leq OEMe \leq 1 \tag{6}$$

$$WMI = (OEFe + OEMe)/2, 0 \leq WMI \leq 1 \tag{7}$$

where"$P_{imp}(t)$" and "$P_{exp}(t)$" are the interaction power of importation and exportation with the grid, respectively. "$t1$" and "$t2$", which respectively represents the integral's lower and upper limits, are the start and end point of the studied period. The "$L_{elec}(t)$" is the sum-up electric power demand of each building including the cooling and heating system and the building operational equipment without the B2V demand of EVs. The "$P_{B2V}(t)$" is the B2V power demand to charge the local EVs. The"$P_{REe}(t)$" refers to the power generated by building REe generation systems, which includes BIPVs, FPVs and/or the wind turbines.

Moreover, two criteria will be applied to study the interactions of the B2V and the V2B of each building. As presented below Eq., "E_{B2V}" refers to the electricity transferred from the building to the EV annually, and "E_{V2B}" represents the annual electricity discharged from EV to building through the EV-integrated system.

$$E_{B2V} = \int_{t1}^{t2} P_{B2V}(t)dt \tag{8}$$

$$E_{V2B} = \int_{t1}^{t2} P_{V2B}(t)dt \tag{9}$$

where the"$P_{B2V}(t)$" is the charging power for the EV batteries, and the "$P_{V2B}(t)$" represents the discharging power of EV batteries to meet building energy demands.

Additionally, in order to examine the interactions between two sharing methods—micro-grid and local EV sharing—three criteria are employed to evaluate each method separately. For micro-grid sharing mode, "E_{O2R_MG}" and "E_{R2O_MG}" show the total shared electricity value from office building to residential building and the opposite sharing direction by micro-grid in a year, respectively. "P_{O2R_MG}" and "P_{R2O_MG}" indicate the sharing power from office to residence and inverse direction by micro-grid in each time step. "E_{B2B_MG}" is the sum-up value of "E_{O2R_MG}" and "E_{R2O_MG}" to show the total energy sharing amount by the micro-grid. For local EV sharing, three indices are used similarly to the micro-grid sharing. "E_{O2R_LEV}" indicates that the total amount of electricity transferred in a year by charging local EVs from the office building then discharging it to the residential building. "P_{O2R_LEV}" is the energy sharing power from office to residence by two EVs which is defined by based on the cumulative charging energy proportion inside the EV batteries that have been charged from the office building in the past, to determine the ratio of the office-to-residence shared energy being discharged in the residential building in each time step. "P_{R2O_LEV}" represents the sharing power from residence to office with alike logic as "P_{O2R_LEV}". "E_{R2O_LEV}" indicates the inverse electricity sharing from the residential building to the office building with similar sharing calculations method as "E_{O2R_LEV}". The total annual electricity sharing amount under local EV sharing mode is presented as "E_{B2B_LEV}" as following Eq.:

$$E_{O2R\_MG} = \int_{t1}^{t2} P_{O2R\_MG}(t)dt \tag{10}$$

$$E_{R2O\_MG} = \int_{t1}^{t2} P_{R2O\_MG}(t)dt \tag{11}$$

$$E_{B2B\_MG} = E_{O2R\_MG} + E_{R2O\_MG} \tag{12}$$

$$E_{O2R\_LEV} = \int_{t1}^{t2} P_{O2R\_LEV}(t)dt \tag{13}$$

$$E_{R2O\_LEV} = \int_{t1}^{t2} P_{R2O\_LEV}(t)dt \tag{14}$$

$$E_{B2B\_LEV} = E_{O2R\_LEV} + E_{R2O\_LEV} \tag{15}$$

Lastly, this study employs the net present value (NPV) as the primary economic indicator to examine the influence of different renewable energy combinations and energy-sharing methods on the financial viability of hybrid systems. Specifically, the NPV considered is the absolute value of the net cash flows from the life-cycle costs of the building systems over 20 years, following the payback phase. Therefore, the formula of the absolute NPV of the building system is shown as follows, while the detailed calculation methods are defined in the Ref. [18]:

$$NPV = PRV_{operation} - C_{REe_{ini}} + PRV_{MGshare} - PRV_{BATrep} + PRV_{BATres} \tag{16}$$

where "C_{REe_ini}" is the amount of the initial investment capital of the renewable generation systems.

$$PRV_{operation} = \sum_{t=1}^{N} \frac{(C_{FiT} - C_{bill} - C_{REe_{ini}} \times F_{O\&M})}{(1+i)^t} \tag{17}$$

$$PRV_{MGshare} = \sum_{t=1}^{N} \frac{(C_{MGexp} - C_{MGimp})}{(1+i)^t} \tag{18}$$

$$PRV_{BATrep} = \sum_{j=1}^{j=J} \frac{C_{BAT\_ini}}{(1+i)^{j*l}} \tag{19}$$

$$PRV_{BATres} = C_{BAT\_ini} \times \frac{l_{res}}{l} \times \left(\frac{1}{1+i}\right)^N \tag{20}$$

where the "C_{FiT}" is the income of the Feed-in tariff for the annual total generation of renewable systems given by the Hong Kong government [52], and the "C_{bill}" is the electricity bill in one year due to the importation from the grid based on a simple constant import tariff 1.5440 HKD/kWh [53]. The "$F_{O\&M}$" represents the ratio of annual operation and maintenance costs to the initial investment in renewable energy, with specific details provided in Table 8. "N" represents the considered system lifetime period of 20 years. The "$PRV_{MGshare}$" is the present value result of micro-grid sharing, which is only activated in micro-grid sharing mode and may be positive or negative, based on whether there is a net import or export through the micro-grid. The "PRV_{BATrep}" is the present value of replacement cost of EV batteries. Other variables such as "l", "j", "J" are lifetime, specific replacement instance and total

Table 8
Economic index of the REe generation systems.

Components	BIPV [54]	FPV [55]	Wind turbine [16]	EV & Building battery [42]	Micro-grid
Initial cost	6227 HKD/kW	26,520 HKD/kW	39,837 HKD/kW	266,163 HKD/unit	16,640 HKD/30 m
O&M ratio of initial cost	1.20 %	1.92 %	0.80 %	N.A.	N.A.
Feed-in Tariff in Hong Kong	3 HKD/kWh [52]				
Interest Rate	2.96 % [56]				
USD to HKD exchange rate	7.8 [57]				

number of replacements, respectively. The initial investment of batteries is defined as "C_{BAT_ini}". "PRV_{BATres}" is the present value of the residual battery. "l_{res}" and "i" represent the residual lifetime and the annual interest rate, respectively.

5. Results and discussions

This research aims to thoroughly assess the impact of energy and financial performance enhancement through three energy sharing methods—instantaneous micro-grid-based, predictive micro-grid-based and local EV-based sharing—between two adjacent grid-tied zero-energy buildings equipped with different renewable electricity generation combinations. To facilitate this analysis, five research groups have been established, as detailed in Table 9. According to Table 9, Groups 1–2 and Group 4 encompass 81 options for renewable electricity generation. Each building has nine combinations of renewable electricity generation systems as illustrated in Table 10, so each group of Groups 1–2 and 4 has a total of 81 combinations. Group 3 is established for two purposes, for Group 3.1 is to study the impact of adding one building battery in residence, while another Group 3.2 is to analyze the impact of the predictive control method. For each combination of REe options, the unit numbers of BIPVs only have two kinds of status, fully installed on the roof (235 units) or none, while the unit numbers of FPVs and wind turbines range from zero to maximum which fully covers the entire annual demand of each building. In terms of differences among Groups 1 to 4: In Group 1, neither the functionality of "EV-based sharing" with V2B capability nor the implementation of "Micro-grid-based sharing" is operational; whereas in Group 2, solely the "Instantaneous Micro-grid-based sharing" is activated, whereas "EV-based sharing" remains inactive; in the subsequent Group 3.1, one residential building battery is added based on Group 2, while the micro-grid-based sharing control is still instantaneous; for Group 3.2, the predictive micro-grid-based control is applied based on Group 3.2; and finally, in Group 4, the "EV-based sharing" is operational, but there is an absence of "Micro-grid-based" sharing. In addition, this study incorporates a baseline reference case designated as "Ref," which excludes any REe generation system. In this reference scenario, neither the "Micro-grid-based sharing" nor the "EV-based sharing" is operational or activated.

Fig. 8 presents a flowchart outlining the research steps. Initially, Section 5.1 delves into the influence of various combinations of renewable electricity (REe) generation systems. In the following Section 5.2.1, the enhancement of the instantaneous micro-grid-based energy-sharing of various renewable combinations is presented. The brief studies about the trading business model of these two buildings are introduced in the subsequent Section 5.2.2. Thereafter, Section 5.3.1 introduces the comparison results between the instantaneous micro-grid-based energy-sharing control with and without the residential building battery and the predictive micro-grid-based sharing, followed by Section 5.3.2 presenting the impact of the trading under predictive micro-grid-based sharing. Then Section 5.4.1 explores how the local EV-based sharing method influences the building compound system and the interactions between the building and vehicles. In Section 5.4.2, the impact of the trading price on net present value is analyzed. In the end, the comparison between the three sharing methods is introduced in Section 5.5. Fig. 8 displays the involvement of research groups 1–4, as detailed in Table 9, for each section discussed. Additionally, it outlines the analysis criteria previously presented in Section 4. To evaluate the technical performance of the building hybrid system, the assessment focuses on annual matching capabilities, which include "OEFe," "OEMe," and "WMI." The evaluation of building-vehicle interactions primarily considers criteria related to interactive energy ("E_{B2B_MG}", "E_{O2R_MG}", "E_{R2O_MG}", "E_{B2B_LEV}", "E_{O2R_LEV}" and "E_{R2O_LEV}"). It is worth noting that the EV schedules of parking positions, commuting, and parking time will impact the V2B functionality.

5.1. *The impact of the hybrid REe systems*

The combined simulation results of all 81 cases in Group 1 about the annual technical and economic performance are listed in Fig. 9. In addition, the best and worst cases regarding the WMI and NPV as well as the reference case are also illustrated in Table 11 for analysis.

Fig. 9 shows that the total WMI index, which measures the matching capabilities of all scenarios in Group 1 without energy sharing between buildings, ranges from 0.463 to 0.692. This variation indicates that different combinations of renewable energy sources significantly affect the matching performance of the building hybrid system. As shown in Table 11, Cases 60, 15, and 55can achieve the top 3 best matching results, more than 14.52 % higher than the average WMI values of all cases. The renewable generation systems of these cases are mainly supported by the wind turbines (from 7 to 11 units) since the renewables generation profile combined majorly by wind turbines and minorly by PVs can better consist with the buildings' demand profile. On the contrary, Cases 31, 36, and 76 show poor technical performance (over 23 % below the average) resulting from the high proportion of PV-supported REe generation systems. The nature of PV generation determines the building can only import electricity from the grid at nighttime and produce more electricity than demand in the daytime, resulting in lower OEFe and OEMe values. On the economic aspect of all cases in Group 1, Cases 5, 1, and 41 acquire the top 3 largest NPV values, over 90 % higher than the average NPV values. The majority of the renewable generation in these cases is powered by wind turbines (from 11 to 13 units). Due to the relatively low investment and maintenance cost per kw capacity of wind turbines compared to PV, the cases with more wind turbines tend to achieve a better performance in the economic aspect. As above-mentioned owing to the consistency of the combined renewable generation profile and the building demand profile, the cases completely powered by the wind turbines do not have the matching capabilities as good as the cases mixed with a large proportion of wind turbines and a small proportion of PV renewable generation. It turns out that the cases with large proportions of wind turbine renewables but not 100 % wind

Table 9
The variables explored in this research.

	REe option	B2V function	V2B function	Instantaneous micro-grid-based energy-sharing	Predictive micro-grid-based energy-sharing	Local EV-based energy-sharing	Residential building battery
Case: Ref	None	Y	N	N	N	N	N
Group 1	BIPV+FPV + WT	Y	N	N	N	N	N
Group 2	BIPV+FPV + WT	Y	N	Y	N	N	N
Group 3.1	BIPV+FPV + WT	Y	N	Y	N	N	Y
Group 3.2	BIPV+FPV + WT	Y	N	N	Y	N	Y
Group 4	BIPV+FPV + WT	Y	Y	N	N	Y	N

Table 10
Combinations of renewable electricity (REe) generation systems of office and residential buildings.

	Office	Office BIPV	Office FPV	Office WT	Residence	Residential BIPV	Residential FPV	Residential WT
Case 1–9	**Combination 1**	235	0	11	**Combination 1**	235	0	11
Case 10–18	**Combination 2**	235	465	7	**Combination 2**	235	494	7
Case 19–27	**Combination 3**	235	981	3	**Combination 3**	235	1010	3
Case 28–36	**Combination 4**	235	1367	0	**Combination 4**	235	1396	0
Case 37–45	**Combination 5**	0	0	13	**Combination 5**	0	0	13
Case 46–54	**Combination 6**	0	154	11	**Combination 6**	0	183	11
Case 55–63	**Combination 7**	0	670	7	**Combination 7**	0	699	7
Case 64–72	**Combination 8**	0	1185	3	**Combination 8**	0	1214	3
Case 73–81								
	Combination 9	0	1572	0	**Combination 9**	0	1601	0

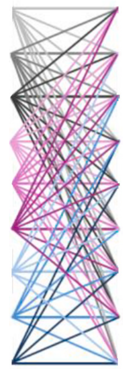

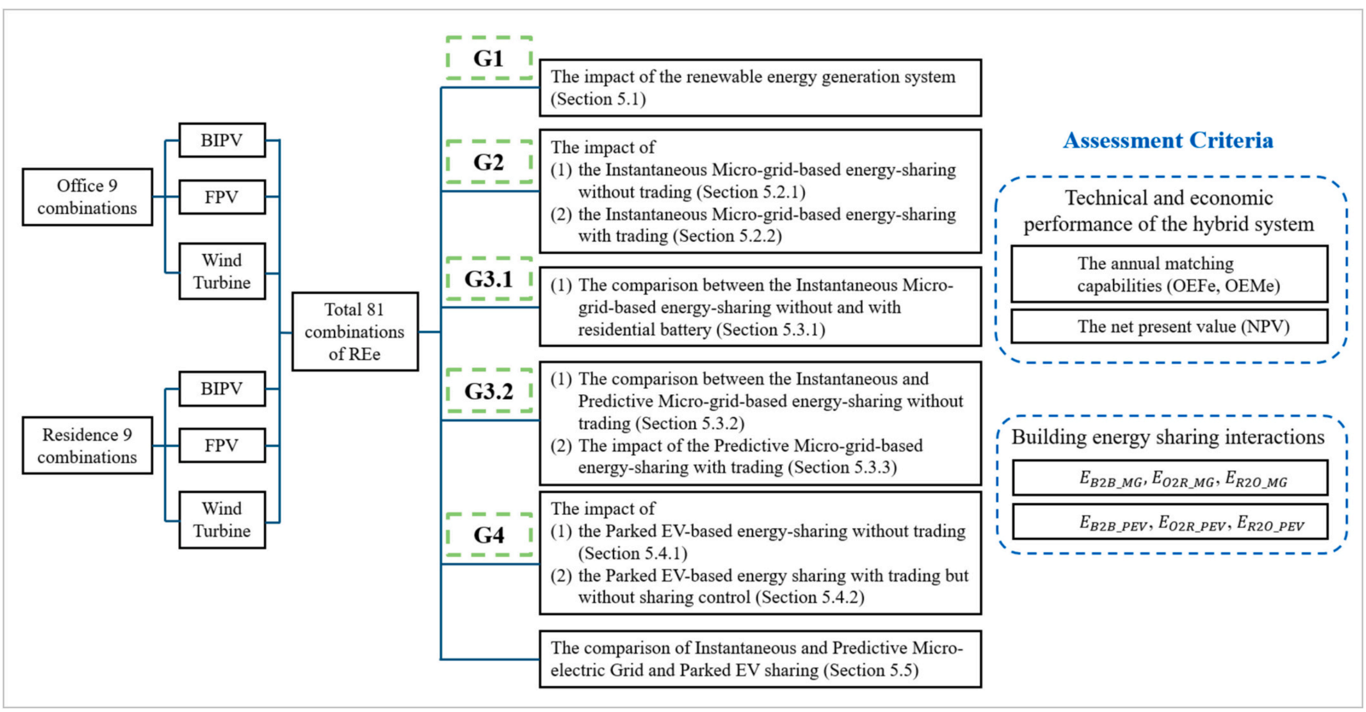

Fig. 8. The flowchart of the research groups, methodology and the analysis criteria. “G1”- “G4” refer to the Groups 1–4 listed in the Table 9.

turbine-supported achieve the best economic performance. On the other hand, Case 81 fully supported by FPV has the poorest economic performance, followed by Case 36 and 76, which are also mainly powered by the FPV. FPV possesses the highest investment cost (26,520 HKD/kW) and annual operational cost (1.92 % of the total investment cost) among the three renewable types, partially resulting in the worst financial outcome. The generation nature of PV also contributes to poor technical performance, causing higher importation and exportation with the grid, which makes the financial outcome even worse. It is worth noting that this economic result may be slightly different in other places because of the different installation and operation costs.

5.2. *The instantaneous micro-grid-based energy-sharing method*

5.2.1. *The impact of the instantaneous micro-grid-based energy-sharing*

To improve the technical and economic efficacy of the building hybrid system, the instantaneous micro-grid-based (Group 2) is introduced to study its impact on energy sharing in this section, followed by the instantaneous micro-grid sharing with residential battery (Group 3.1) and the predictive micro-grid-based sharing analysis (Group 3.2) in Section 5.3. The control strategy of this sharing method is elaborated in previous Section 3.2.1. First, as depicted in Fig. 10 and Table 12, two neighboring buildings sharing excess energy through a connected cable known as a micro-grid result in the total WMI and total NPV for the two buildings in Group 2 averaging increases of 7.19 % and 1,109,602 HKD,

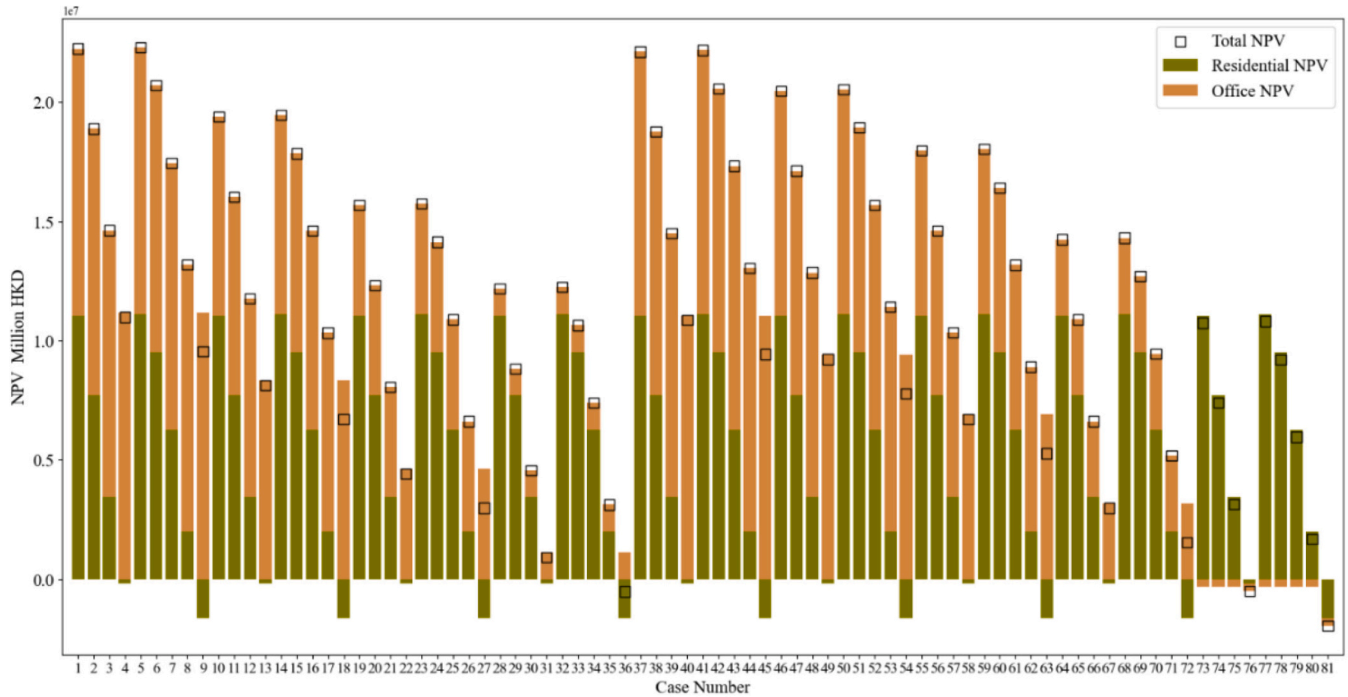

(a)

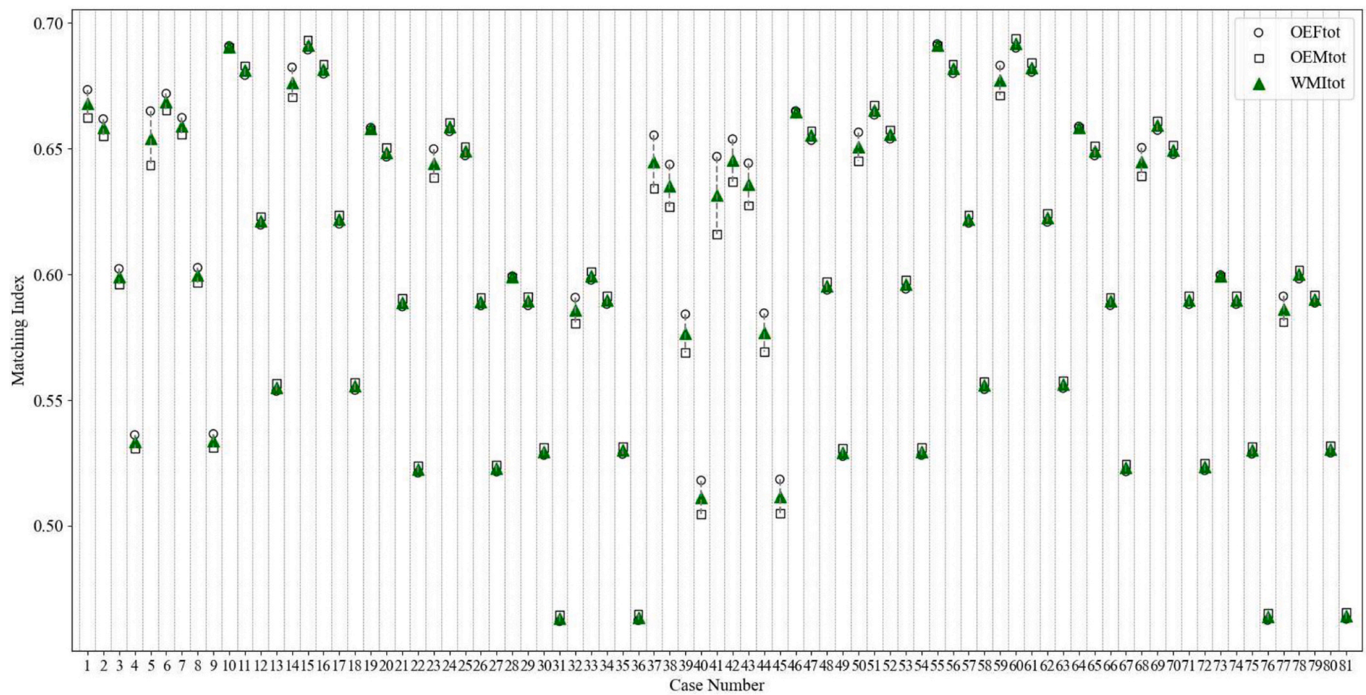

(b)

Fig. 9. Total NPV and total WMI of all 81 combination cases in Group 1. (a) Total NPV of all 81 combination cases, and (b) Total WMI of all 81 combination cases.

respectively, across 81 cases compared to Group 1. The OEFe and OEMe values, which serve as indicators to illustrate the technical performance of building systems as mentioned in Section 4, also show the simultaneous improvement in the WMI index of both buildings. Activating energy sharing through the micro-grid, it enhances the use of generated renewable energy, decreasing the necessity to import and export electricity from the external grid. This results in improved OEFe, OEMe, and WMI for all cases in Group 2. The improvement of the total WMI by instantaneous micro-grid sharing ranges from 0.97 % to 33.59 % depending on the renewable energy generation combinations of each building. Cases 45, 40 and 54 represent the largest enhancement of WMI from 26.75 % to 33.59 % by the micro-grid as presented in Table 12. For these cases that have more wind turbines on one side, especially the office side and all PVs on the other residence side, the micro-grid serves

Table 11
Typical top and worst 3 cases of total NPV and total WMI in Group 1.

	Case number	Office			Residence			Technical performance			Economic performance		
		Number of BIPV	Number of FPV	Number of WT	Number of BIPV	Number of FPV	Number of WT	Total OEF	Total OEM	Total WMI	Office NPV (HKD)	Residence NPV (HKD)	Total NPV (HKD)
Top 3	60	0	670	7	0	183	11	0.690	0.694	0.692	6,903,488	9,514,764	16,418,252
WMI	15	235	465	7	0	183	11	0.689	0.693	0.691	8,332,914	9,514,764	17,847,677
cases	55	0	670	7	235	0	11	0.692	0.691	0.691	6,903,488	11,056,104	17,959,592
Top 3	5	235	0	11	0	0	13	0.665	0.643	0.654	11,182,637	11,122,898	22,305,536
NPV	1	235	0	11	235	0	11	0.673	0.662	0.668	11,182,637	11,056,104	22,238,741
cases	41	0	0	13	0	0	13	0.647	0.616	0.631	11,053,936	11,122,898	22,176,834
Worst 3	31	235	1367	0	235	1396	0	0.462	0.464	0.463	1,129,045	−194,206	934,839
WMI	36	235	1367	0	0	1601	0	0.462	0.465	0.464	1,129,045	−1,630,466	−501,420
cases	76	0	1572	0	235	1396	0	0.462	0.465	0.464	−305,471	−194,206	−499,677
Worst 3	81	0	1572	0	0	1601	0	0.463	0.465	0.464	−305,471	−1,630,466	−1,935,936
NPV	36	235	1367	0	0	1601	0	0.462	0.465	0.464	1,129,045	−1,630,466	−501,420
cases	76	0	1572	0	235	1396	0	0.462	0.465	0.464	−305,471	−194,206	−499,677

as a powerful tool for the office side to share its energy surplus generated by wind turbines at night to meet the demand of the residential side without any renewable energy at night. In contrast to the great improvements, Cases 76, 31 and 81 fully powered by the PV show the poorest technical improvements by micro-grid. The mismatching characteristics between the PV generation nature and the building demand in these cases are hard to optimize significantly by instantaneous micro-grid sharing, since the micro-grid can only conduct instant sharing.

As for the economic performance of Group 2, similar results align with the technical outcomes. The top 3 largest enhancement cases of NPV presented in Table 12 correspond with the WMI improvement cases, ranging from 3,096,741 HKD to 3,764,380 HKD. Both WMI and NPV improvements chiefly attribute to the increasing utilization of the wind turbine surplus generation from the office side to the residential side at nighttime as well as the PV surplus generation from the opposite direction in the daytime, saving much imported energy and electricity bills. The energy flow of one typical week of top WMI and NPV Case 45 is selected to demonstrate in Fig. 11 about how night-time office surplus generated by wind turbine and day-time residential surplus generated by PV is utilized by the micro-grid sharing to improve building performance of both sides. Cases 40 and 54 are two typical cases to show that one of the building's NPV switch from negative to positive when the micro-grid is applied, indicating that the instantaneous micro-grid sharing is capable of changing some cases from non-profitable to financially feasible. These cases also show that when two neighboring buildings are equipped with complementary renewable generation systems, the micro-grid can greatly enhance their both technical and economic performance. However, the micro-grid shows weak economic enhancement down to 246,448 HKD when two buildings have similar combinations as presented in Cases 1, 76 and 81 in Table 12. The matching performance of Case 1 without micro-grid sharing already reaches a good level, therefore the micro-grid sharing improvement is limited. Cases 76 and 81 are the typical cases to indicate micro-grid can bring negative results for one of the buildings compared to those without micro-grid, due to its improvement on matching cannot compensate for the added investment cost of the micro-grid cable. It can also be further concluded from the energy sharing amount between two buildings that the increasing renewables combination diversity brings higher micro-grid sharing amount, particularly those cases with one building supported solely by wind turbines and another supported only by PVs. Consequently, higher micro-grid sharing value means less energy being imported and exported, therefore leading to better improvements in technical and economic performance.

5.2.2. The impact of the instantaneous micro-grid-based trading business model

As concluded in Section 5.2.1, the technical and economic performance of two neighboring buildings can be improved by connecting them with a micro-grid cable. However, these two buildings are owned by two different stakeholders, therefore it is reasonable to consider the trading price between these two buildings for the instantaneous micro-grid-based sharing. As mentioned in previous Section 3.2, the energy control system transfers energy between buildings by micro-grid whenever it is possible. The trading price for energy sharing is the same for both stakeholders based on mutual agreement and ranges from 0 to a maximum of 1.5 HKD per kWh, taking into account that the trading price should not exceed the electricity price of the power grid (1.544 HKD/kWh). Case 5 is selected in Fig. 12 to show the pattern after the trading price application. As the price increases, the NPV of the building receiving more energy annually from another building continues to decrease. The decreasing part of NPV in this building becomes the increasing part of NPV in another building that transfers more energy to micro-grid, while the total NPV remains the same. In this business model, the building with more surplus electricity transferred by micro-grid earns more profits by sharing. On the other hand, the stakeholder of the building receiving more energy by micro-grid pays more for the energy sharing. However, it is still profitable for this stakeholder due to the lower price of micro-grid trading compared to the power grid price.

5.3. The predictive micro-grid-based energy-sharing method

5.3.1. The comparison between the instantaneous micro-grid-based energy-sharing method without and with residential battery and predictive micro-grid-based energy-sharing method

Based on the instantaneous micro-grid-based energy-sharing method of Group 2, one extra battery is added to the residential building in Group 3.1 to better compare the performance between the instantaneous micro-grid-based sharing and predictive micro-grid-based sharing, as presented in Table 9. The instantaneous micro-grid-based energy-sharing control with added residential building battery is the same as the predictive micro-grid-based energy-sharing control except that the instantaneous one does not have DMI control. The detailed control strategies and differences of these two strategies are described in above Section 3.2.2. Three typical cases such as Case 5 (Top NPV performance), Case 45 (Top Enhancement) and Case 76 (Worst Enhancement) are selected in Table 13 to demonstrate the general trend of impact brought by the added residential building battery on the instantaneous micro-grid-based sharing. All three cases show positive on both WMI (from 3.65 % to 11.52 %) and NPV (from 21,076 HKD to 271,479 HKD) enhancement on residence side. The residential building battery served as an energy storage contributes to higher utilization of renewable generation, providing time-shift ability for energy usage, therefore resulting in better matching capability. On the other hand, the added residential battery brings negative effect on both technical and economic aspect of office building from −0.29 % to −1.79 %, since the

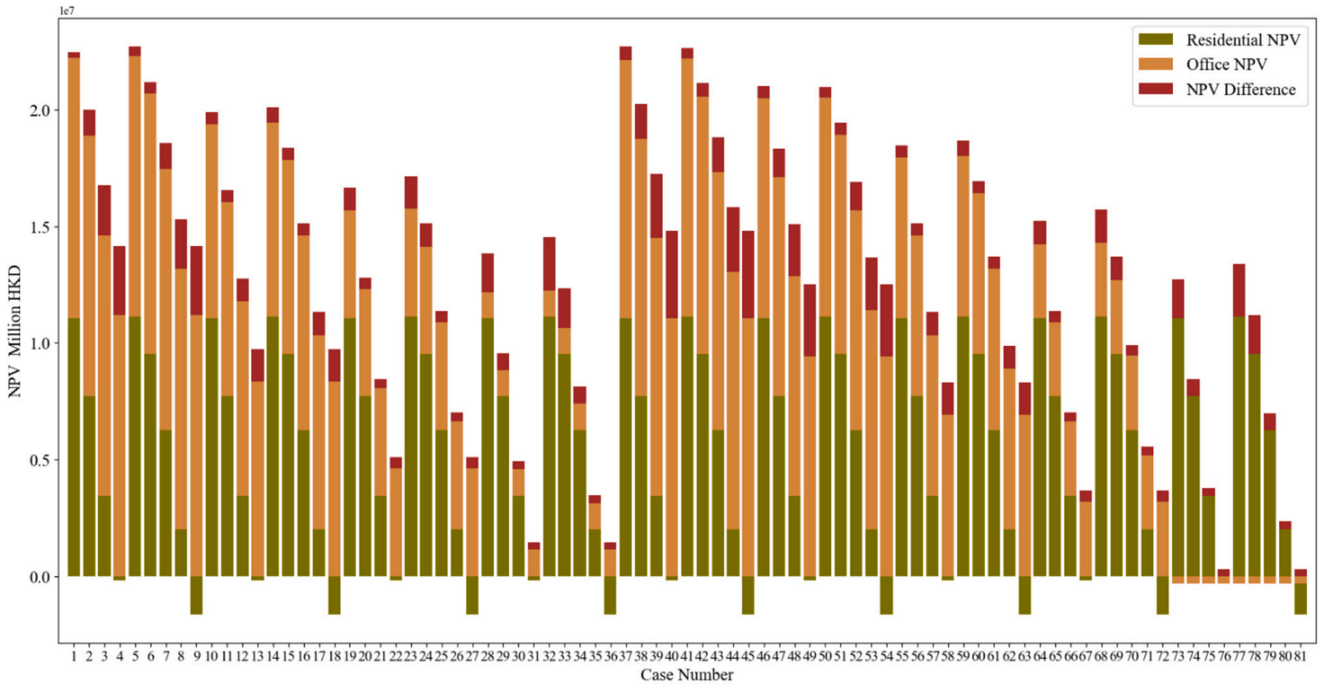

(a)

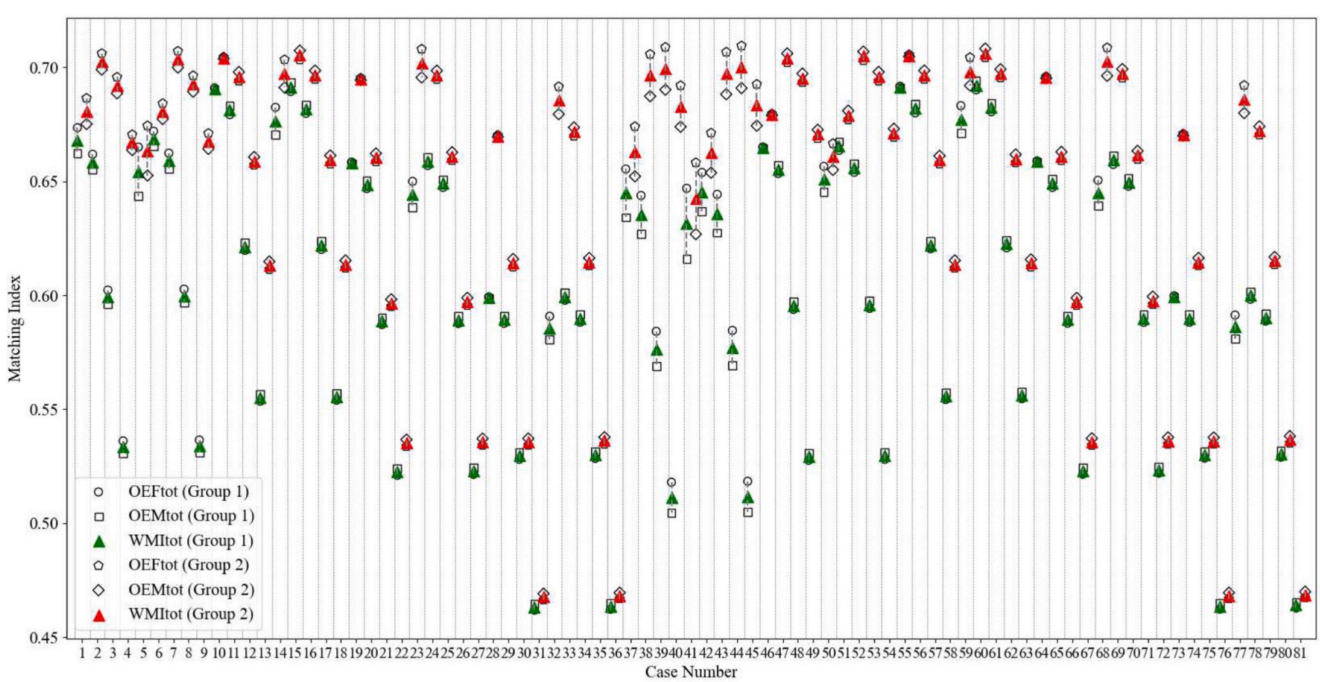

(b)

Fig. 10. The NPV and technical performance improvement with and without instantaneous micro-grid-based sharing of all 81 combination cases in Group 2. (a) Total NPV improvement with and without instantaneous micro-grid-based sharing of all 81 combination cases, and (b) Technical performance improvement with and without instantaneous micro-grid-based sing of all 81 combination cases.

residential battery stores or discharges some energy which is supposed to be transferred to or from office under instantaneous micro-grid-based control. In general, three cases show positive technical improvement, while only the worst enhancement Case 76 shows that the overall technical improvement does not guarantee a better total economic performance unless the residential NPV increasement outnumbers the office NPV reduction.

Case 5 has the largest total NPV and the renewables investment on both buildings is considered financially feasible, so it is selected as the typical case to demonstrate the technical and economic impact of predictive micro-grid-based sharing control. As shown in Table 14, two extrema and one middle trading price are chosen to compare the differences between the instantaneous micro-grid-based energy-sharing method without residential battery (Group 2), with residential battery

Table 12
Top and worst 3 enhancement cases of total NPV and total WMI under instantaneous micro-grid-based sharing respectively in Group 2.

	Case number	Renewable combinations						Technical performance										Economic performance			
		Office			Residence			Office			Residence			Total				Office	Residence	Total	
		Number of BIPV	Number of FPV	Number of WT	Number of BIPV	Number of FPV	Number of WT	Office OEF	Office OEM	Office WMI	Residential OEF	Residential OEM	Residential WMI	Total OEF	Total OEM	Total WMI	Enhancement rate	Office NPV (HKD)	Residence NPV (HKD)	Total NPV (HKD)	Enhancement value (HKD)
Top 3 WMI	45	0	0	13	0	1601	0	0.789	0.798	0.794	0.597	0.545	0.571	0.692	0.674	0.683	33.59 %	12,786,528	401,322	13,187,850	3,764,380
enhancement	40	0	0	13	235	1396	0	0.789	0.798	0.793	0.596	0.544	0.570	0.692	0.674	0.683	33.59 %	12,782,353	1,838,936	14,621,289	3,761,560
cases	54	0	154	11	0	1601	0	0.779	0.833	0.806	0.562	0.516	0.539	0.669	0.673	0.671	26.75 %	10,840,999	39,109	10,880,107	3,096,741
Top 3 NPV	45	0	0	13	0	1601	0	0.789	0.798	0.794	0.597	0.545	0.571	0.692	0.674	0.683	33.59 %	12,786,528	401,322	13,187,850	3,764,380
enhancement	40	0	0	13	235	1396	0	0.789	0.798	0.793	0.596	0.544	0.570	0.692	0.674	0.683	33.59 %	12,782,353	1,838,936	14,621,289	3,761,560
cases	54	0	154	11	0	1601	0	0.779	0.833	0.806	0.562	0.516	0.539	0.669	0.673	0.671	26.75 %	10,840,999	39,109	10,880,107	3,096,741
Worst 3 WMI	76	0	1572	0	235	1396	0	0.537	0.533	0.534	0.398	0.407	0.403	0.467	0.469	0.468	0.97 %	19,413	−199,672	−180,259	319,418
enhancement	31	235	1367	0	235	1396	0	0.536	0.532	0.534	0.398	0.408	0.403	0.466	0.469	0.468	0.98 %	1,454,405	−199,930	1,254,475	319,636
cases	81	0	1572	0	0	1601	0	0.537	0.532	0.535	0.399	0.408	0.404	0.467	0.470	0.469	0.98 %	21,049	−1,636,600	−1,615,551	320,385
Worst 3 NPV	1	235	0	11	235	0	11	0.691	0.673	0.682	0.682	0.677	0.679	0.686	0.675	0.681	1.92 %	11,317,780	11,167,409	22,485,189	246,448
enhancement	76	0	1572	0	235	1396	0	0.537	0.533	0.535	0.398	0.407	0.403	0.467	0.469	0.468	0.97 %	19,413	−199,672	−180,259	319,418
cases	31	235	1367	0	235	1396	0	0.536	0.532	0.534	0.398	0.408	0.403	0.466	0.469	0.468	0.98 %	1,454,405	−199,930	1,254,475	319,636
Average				/				0.686	0.677	0.682	0.611	0.615	0.613	0.648	0.646	0.647	7.19 %	6,875,112	5,878,860	12,753,972	1,109,602

(Group 3.1) and predictive micro-grid-based energy-sharing method (Group 3.2). As previously mentioned in Section 3.2.2, unlike the instantaneous micro-grid-based control, the predictive micro-grid-based control is designed for the financial benefit of residential stakeholder by controlling the shared energy amount from office side. When there is no trading price of micro-grid sharing, the DMI_R is always equal or greater than 0.5, therefore the predictive micro-grid-based control is the same as the instantaneous micro-grid-based control with residential battery. With the trading price increases, the residence uses DMI_R to control the amount of shared energy, resulting in an increasing deterioration on both buildings' matching capabilities, while the decreasing sharing amount has more impact on office building side than residence. The detailed trading price analysis on technical and economic performance is presented by Case 5 in the following Section 5.3.2.

Fig. 13 (a) and (b) display the outcome difference around Time 880 h. It demonstrated the impact of DMI_R by comparing the residential building energy flow between two extrema of the trading price of the typical two-day period (February 5th-February 7th). As shown in Fig. 13 (a), DMI_R exceeds 0.5 for two days when trading price is at minimum 0.1 HKD. Therefore, when there is a shortage of residence at around hour 880, it is first met by adopting the sharing power from the office. However, at the same time in Fig. 13(b) when the trading price reaches 1.5 HKD, the residential building discharges the residential battery to meet the shortage first instead of transferring power from the micro-grid due to low DMI_R. In these two cases, though by definition the DMI_R is determined by both trading price and future energy conditions, the selection of extrema trading price weakens the impact of future energy conditions on the index.

5.3.2. *The impact of the predictive micro-grid-based trading business model*

As the trading price augments, the annual electricity sharing amount by the micro-grid from office to residence (as indicated by MGO2R in Fig. 14 decreases, especially when the trading price is larger than 0.40 HKD. When the price is 1.50 HKD, the MGO2R almost reaches zero, showing that the price control factor is functioning, and it is not as economical as low trading price cases for the residential building to receive electricity from the office in high trading price cases. The technical performance of the office building indicated by WMI-O shows the matching capability deteriorates while the trading price rises. The principal factor is the growing exportation of surplus renewable electricity, driven by decreased micro-grid sharing from office buildings to residential ones. However, residential WMI, which is an average value of OEF-R and OEM-R, shows a different trend of small fluctuations first then a downward trend. The decreasing OEF-R illustrates an increase in the amount of imported electricity, while the improvement in OEM-R presents a higher utilization rate of renewable energy as the trading price enlarges. The combination of these two variables' changes leads to the result of WMI-R.

Moreover, the economic performance of the office illustrated by the NPV index indicates an upward trend first then a downward trend as the trading price increases. The office NPV reaches a peak point at 0.5 HKD. On the other hand, the residential NPV shows the opposite trend of downward trend first then the upward trend. The going upward trend of office comes from the larger micro-grid sharing profits within low trading price ranges below 0.50 HKD. After the trading price exceeds 0.50 HKD, the gap between the office and residential sharing profits reduces and eventually the residential sharing profits overtake, since the predictive control of micro-grid sharing only focuses on the MGO2R and with very limited influence on MGR2O. What's more, by applying the residential micro-grid sharing predictive control, it is not financially attractive for office stakeholders. The added residential battery expands the flexibility of residential energy management but unavoidably reduces the transfer of the surplus renewable energy to the office side due to battery self-storage, therefore these reductions must be imported by the office and bring higher electricity bills. Nonetheless, the impact of predictive control on the residential building varies from different

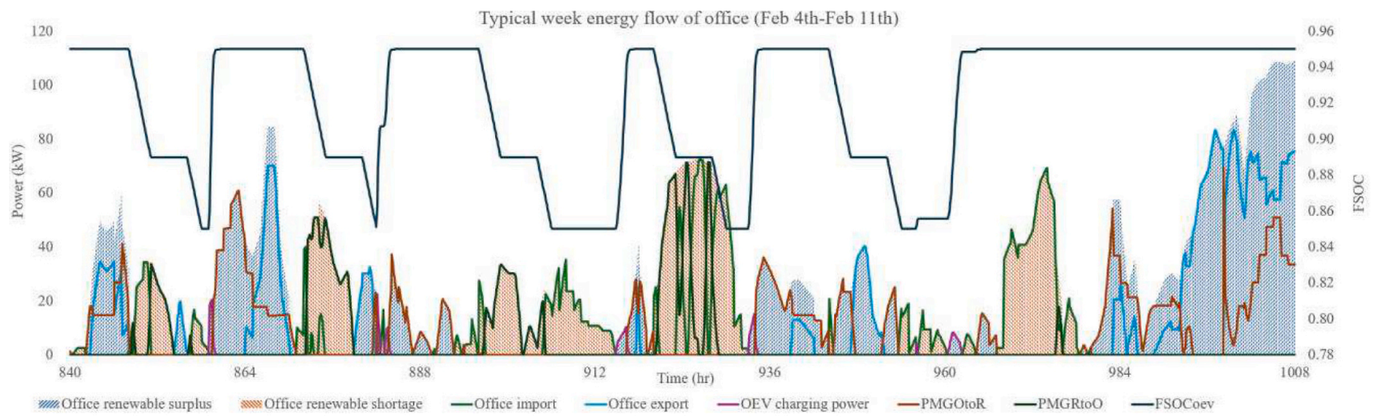

(a)

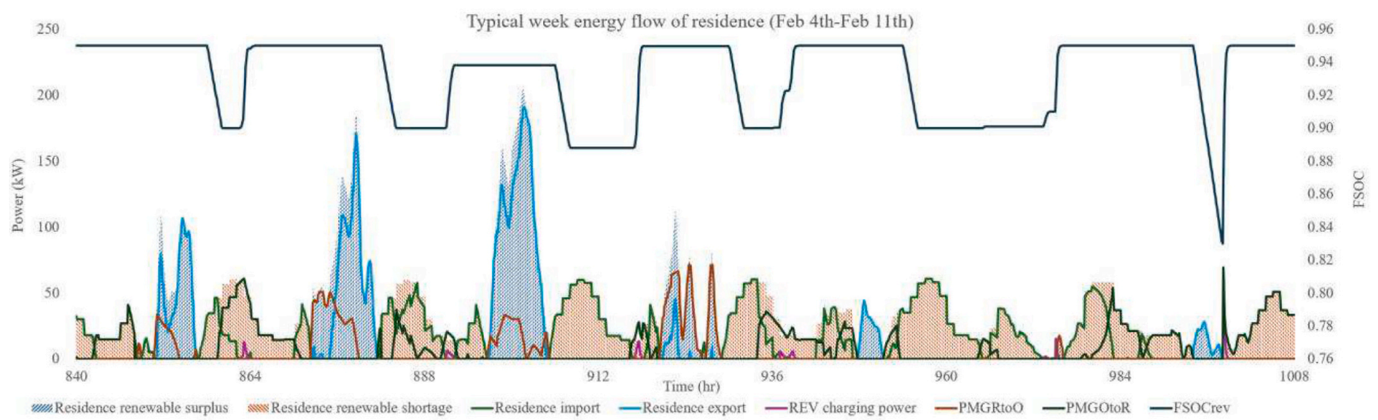

(b)

Fig. 11. Case 45: Typical week energy flow of two buildings from February 4th to February 11th. Time 840–864 means the first day (Monday) of the typical week. "PMGOtoR" means the sharing power from office to residence, and "PMGRtoO" means the sharing power from residence to office. (a) Office building, and (b) Residential building.

trading prices as shown in Fig. 15. In this selected Case 5 as depicted in Fig. 15(b), the residential NPV unveils a U-shape profile, which continues to drop as the trading price is going up until the price equals 1.30 HKD with the exception at 1.00 HKD, then it climbs again. When the trading price is lower than 0.90 HKD, the reasons of residential NPV drop come from both the increase in electricity import and the trading fee of higher micro-grid sharing from office to residential. However, the residential NPV still shows better performance when trading price

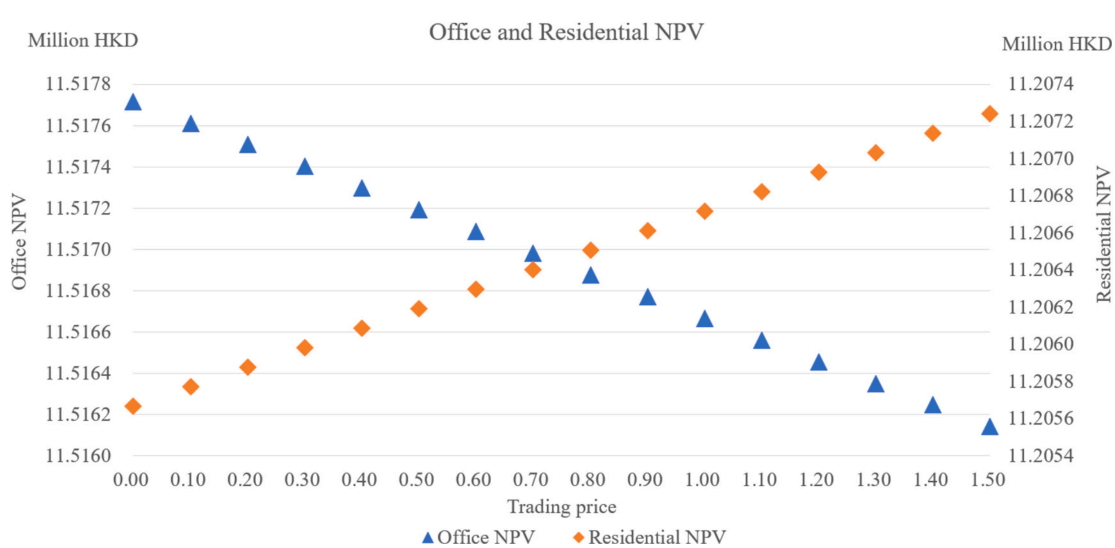

Fig. 12. Office and residential NPV change with different trading prices under instantaneous micro-grid-based sharing.

Table 13
The comparison of three selected cases in instantaneous micro-grid-based control (Group 2) and instantaneous micro-grid-based control with residential battery (Group 3.1).

		Renewable combinations							Technical performance									Economic performance		
	Case number	Office			Residence				Office			Residence			Total			Office	Residence	Total
		Number of BIPV	Number of FPV	Number of WT	Number of BIPV	Number of FPV	Number of WT		Office OEF	Office OEM	Office WMI	Resid-ential OEF	Resid-ential OEM	Resid-ential WMI	Total OEF	Total OEM	Total WMI	Office NPV (HKD)	Residen-ce NPV (HKD)	Total NPV (HKD)
Top NPV case	5	235	0	11	0	0	13	Instantaneous micro-grid-based control	0.687	0.669	0.678	0.662	0.636	0.649	0.674	0.652	0.663	11,273,135	11,205,665	22,478,800
								Instantaneous micro-grid-based control with residential battery	0.683	0.669	0.676	0.688	0.660	0.674	0.685	0.664	0.675	11,229,184	11,226,741	22,455,925
								Change rate/ amount	−0.61 %	0.00 %	−0.31 %	3.75 %	3.55 %	3.65 %	1.59 %	1.79 %	1.69 %	−43,951	21,076	−22,875
Top Enhance-ment case	45	0	0	13	0	1601	0	Instantaneous micro-grid-based control	0.789	0.798	0.794	0.597	0.545	0.571	0.692	0.674	0.683	12,541,946	401,322	12,943,268
								Instantaneous micro-grid-based control with residential battery	0.764	0.796	0.780	0.643	0.573	0.608	0.703	0.687	0.695	12,283,681	624,982	12,908,663
								Change rate/ amount	−3.38 %	−0.26 %	−1.79 %	7.14 %	4.86 %	6.06 %	1.47 %	1.83 %	1.65 %	−258,265	223,659	−34,606
Worst Enhance-ment case	76	0	1572	0	235	1396	0	Instantaneous micro-grid-based control	0.537	0.533	0.535	0.398	0.407	0.403	0.467	0.469	0.468	−225,169	−199,672	−424,841
								Instantaneous micro-grid-based control with residential battery	0.533	0.533	0.533	0.449	0.461	0.455	0.491	0.497	0.494	−257,995	71,807	−186,189
								Change rate/ amount	−0.60 %	0.02 %	−0.29 %	11.39 %	11.65 %	11.52 %	4.93 %	5.47 %	5.20 %	−32,826	271,479	238,653

Table 14
The comparison of three selected trading price cases in instantaneous micro-grid-based control (Group 2), instantaneous micro-grid-based control with residential battery (Group 3.1), and predictive micro-grid-based control (Group 3.2).

Case 5	TP	Office WMI	Change rate	Residential WMI	Change rate	Total WMI	Change rate	MGO2R	MGR2O	Office NPV (HKD)	Change amount	Residential NPV (HKD)	Change amount	Total NPV (HKD)	Change amount
Instantaneous micro-grid-based control	0	0.6780	REF	0.6492	REF	0.6634	REF	2546	2616	11,273,135	REF	11,205,665	REF	22,478,800	REF
Instantaneous micro-grid-based control with residential battery		0.6759	−0.31 %	0.6738	3.79 %	0.6748	1.72 %	3888	2455	11,229,184	−43,951	11,226,741	21,076	22,455,925	−22,875
Predictive micro-grid-based control with residential battery		0.6759	0.00 %	0.6738	0.00 %	0.6748	0.00 %	3888	2455	11,229,184	0	11,226,741	0	22,455,925	0
Instantaneous micro-grid-based control	0.8	0.6780	REF	0.6492	REF	0.6634	REF	2546	2616	11,272,294	REF	11,206,506	REF	22,478,800	REF
Instantaneous micro-grid-based control with residential battery		0.6759	−0.31 %	0.6738	3.79 %	0.6748	1.72 %	3888	2455	11,246,295	−25,999	11,209,630	3123	22,455,925	−22,875
Predictive micro-grid-based control with residential battery		0.6745	−0.20 %	0.6737	−0.01 %	0.6741	−0.10 %	2658	2446	11,233,035	−13,261	11,207,638	−1991	22,440,673	−15,252
Instantaneous micro-grid-based control	1.5	0.6780	REF	0.6492	REF	0.6634	REF	2546	2616	11,271,558	REF	11,207,242	REF	22,478,800	REF
Instantaneous micro-grid-based control with residential battery		0.6759	−0.31 %	0.6738	3.79 %	0.6748	1.72 %	3888	2455	11,261,268	−10,291	11,194,657	−12,585	22,455,925	−22,875
Predictive micro-grid-based control with residential battery		0.6715	−0.65 %	0.6718	−0.29 %	0.6717	−0.46 %	0	2425	11,184,369	−76,899	11,205,510	10,853	22,389,879	−66,046

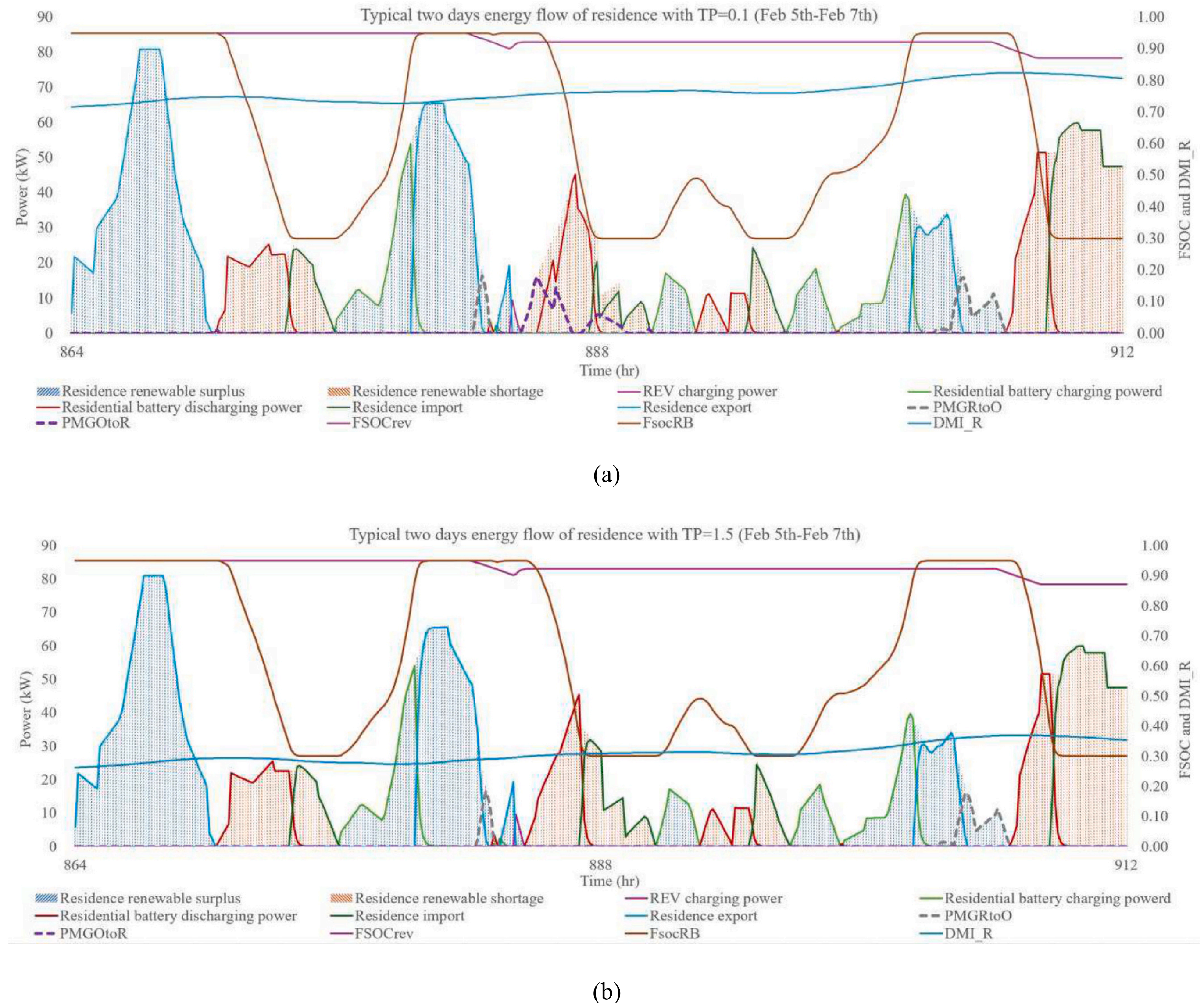

Fig. 13. Case 5: Typical two-day energy flow of residential building from February 5th to February 7th with different trading prices. "PMGOtoR" means the sharing power from office to residence, and "PMGRtoO" means the sharing power from residence to office. (a) Trading price equals 0.1 HKD, and (b) Trading price equals to 1.5 HKD.

ranges in 0.2 to 0.4 HKD compared to the instantaneous micro-grid sharing with residential battery enhanced. The micro-grid trading profits turn positive and start to boost for the residential stakeholder when the trading price exceeds 0.90 HKD. However, the trading profits cannot surpass the rise of the electricity bill until the trading price outruns 1.3 HKD.

In conclusion, based on the abovementioned results, the optimal trading price for the office stakeholder in Case 5 under predictive micro-grid-based control mode is below 0.5 HKD. As for the residential stakeholder, lower trading price shows better economic attractions. To minimize the loss of profits of the office stakeholder as well as maintain positive profit of the residential stakeholder compared to normal instantaneous micro-grid sharing, it is recommended to set the mutual-agreed trading price in a low range. Exploring the integration of building batteries and implementing precise micro-grid predictive control in both buildings presents an intriguing avenue for future research.

5.4. The local electric-vehicle-based sharing method

5.4.1. The impact of the local electric-vehicles-based energy-sharing

As outlined in Section 5.2 and Section 5.3, an analysis of the performance on instantaneous micro-grid-based sharing (Group 2), instantaneous micro-grid-based sharing (Group 3.1) and predictive micro-grid-based sharing (Group 3.2) have been addressed. This section delves into the technical and economic performance of the local electric-vehicle (EV) based sharing method between the two buildings identified as Group 4 in Table 9. The elaborated control strategies and detailed logic are presented in previous Section 3.2.3. The local EV-based sharing does not have any physical electric cable connecting these two buildings, so the energy sharing is purely dependent on the EV charging in one building and discharging in another building. Therefore, unlike the micro-grid-based sharing, the energy sharing between these two buildings is not instantaneous transferred but in time intervals influenced by both EV schedules. Moreover, the EV battery also serves as an energy storage, so it is feasible to regulate the energy surplus and shortage at different times and parked positions. As mentioned in Section 4, the EV battery cycle number is considered in the NPV calculations to analyze

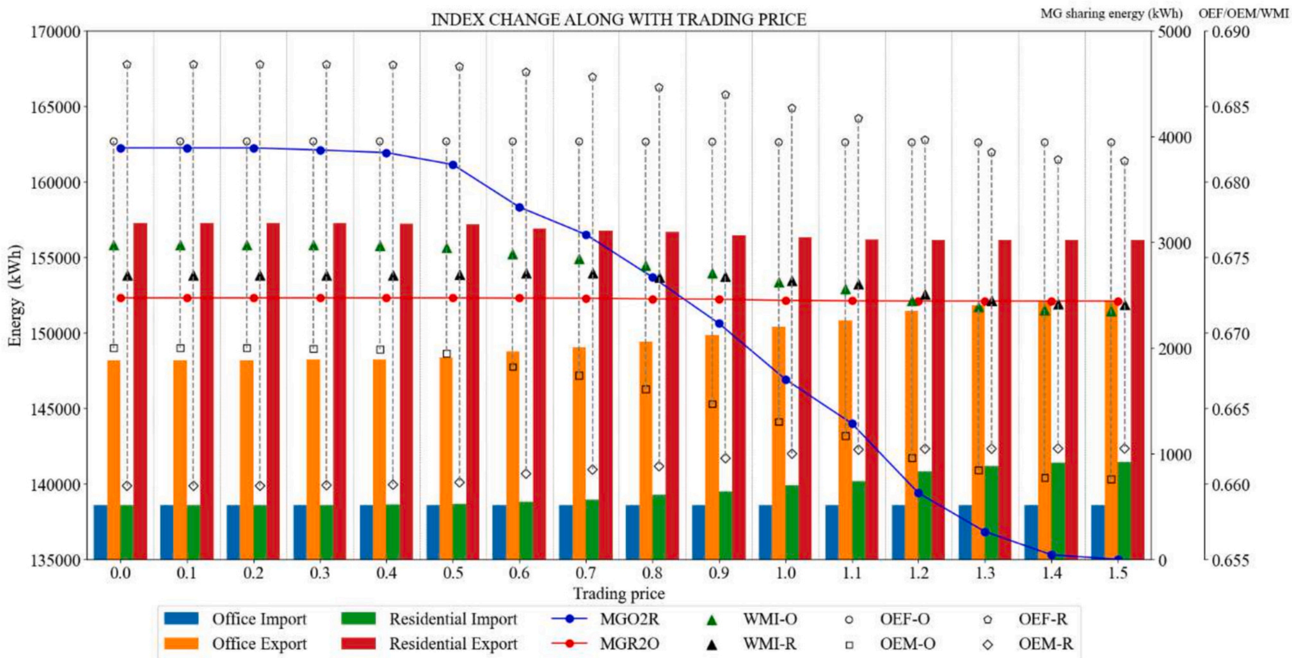

Fig. 14. The relationship between import, export, micro-grid sharing amount and technical performance of two buildings under micro-grid predictive control sharing. "MGO2R" means the annual energy-sharing amount from office to residence. "MGR2O" means the annual energy-sharing amount from residence to office. "WMI-O", "OEF-O" and "OEM-O" refer to the WMI, OEF and OEM index of the office building, respectively. "WMI-R", "OEF-R" and "OEM-R" refer to the WMI, OEF and OEM index of the residential building, respectively.

the impact of battery degradation both in micro-grid-based and local EV-based sharing mode.

Firstly, when two buildings are considered as a united hybrid system, the average technical and economic performance of 81 cases indicated by the total WMI and total NPV increase 6.86 % and 5.70 % compared to Group 1 respectively as shown in Fig. 16 and Table 15. Similar to instantaneous micro-grid-based sharing, the total OEF and OEM also show positive average improvement at 7.66 % and 6.06 %, respectively. The improvement of the total WMI by local EV sharing, ranging from 3.75 % to 12.02 %, is tremendously affected by the renewable energy combinations of the two buildings. As shown in Table 15, Cases 31, 36 and 76 are the typical best WMI improvement cases by local EV-based sharing with an average increase of WMI over 12 %. The EV-based sharing method operates on a mechanism where surplus REe from each building is charged and stored within EVs. This stored energy is subsequently discharged in another building when the EVs switch parking spots. This dynamic results in a time lag effect, enabling the utilization of past surplus energy to address present energy shortages. The time lag resulting from the EV schedule leads to better surplus-shortage energy matching between two buildings when both renewable systems are entirely supported by PVs as shown by Case 31 in Fig. 17. During the typical weekdays, allopatric charging and discharging of two EVs actively increase the energy sharing amount between the two buildings. On the contrary, the cases with renewable systems majorly supported by wind turbines, such as Cases 6, 1 and 51, are less impacted by integrating the local EV-based sharing. The renewable systems have already achieved good matching capabilities without any sharing, so the enhancement of EV-based sharing is limited.

Regarding the economic performance of Group 4, the cases with the office building only powered by PVs and the residential building partially powered by wind turbines have better total NPV improvements above 865,000 HKD as indicated in Cases 80, 35 and 75 in Table 15. The cases with better NPV enhancements have shown a high positive correlation with the cases with better WMI improvements. Cases 80 and 75 are also typical cases in which the NPV of the office building turns from negative to positive when local EV-based sharing is applied, showing that equipping the existing EV with a discharging function in some cases can make the renewables generation system investment from a bad bargain to a financially feasible deal. Conversely, when the office building exhibits a higher proportion of wind-turbine-generated energy, the EV sharing has a limited positive impact on NPV growth as indicated in Table 15. Based on the discussion in Section 5.2, the buildings' renewable combination with a higher proportion of wind turbines can already achieve favorable economic performance in terms of no sharing for their appropriate matching between generation and needs, so there is little room for EV sharing to improve in the economic aspects. It can be further concluded from the energy sharing amount between the two buildings that the residential building shares more energy to the office building by EV, and the higher percentage of PV generation of office buildings results in a higher energy sharing amount from residence to office, and therefore leading to bigger improvements on both technical and economic enhancements.

5.4.2. *The impact of the trading business model*

From previous sections, it is concluded that the local EV-based sharing method has a positive impact on both the technical and economic performance of these two neighboring buildings. Since two buildings have two different stakeholders, they are not obligated to share the electricity for free and tend to gain economic benefits by EV sharing. So in this section, the trading price between two buildings EV sharing is considered. Unlike the instantaneous sharing of micro-grid-based cable that the building receives and consumes energy at the same time, EV sharing has the time-lag effect. It means that the energy storage of the EV battery is mixed with multiple charging and discharging from different charging ports at different times, so it is difficult to differentiate the specific sharing amount from one building to another. In order to understand the sharing trend, as mentioned above in Section 4, the sharing proportion of each EV discharge in another building at this time step is defined as the same proportion of the cumulative own-building-energy-charging in the past. In this section, the trading business model studies the NPV impact after trading price application based on the previous result in Section 5.4.1, and the control

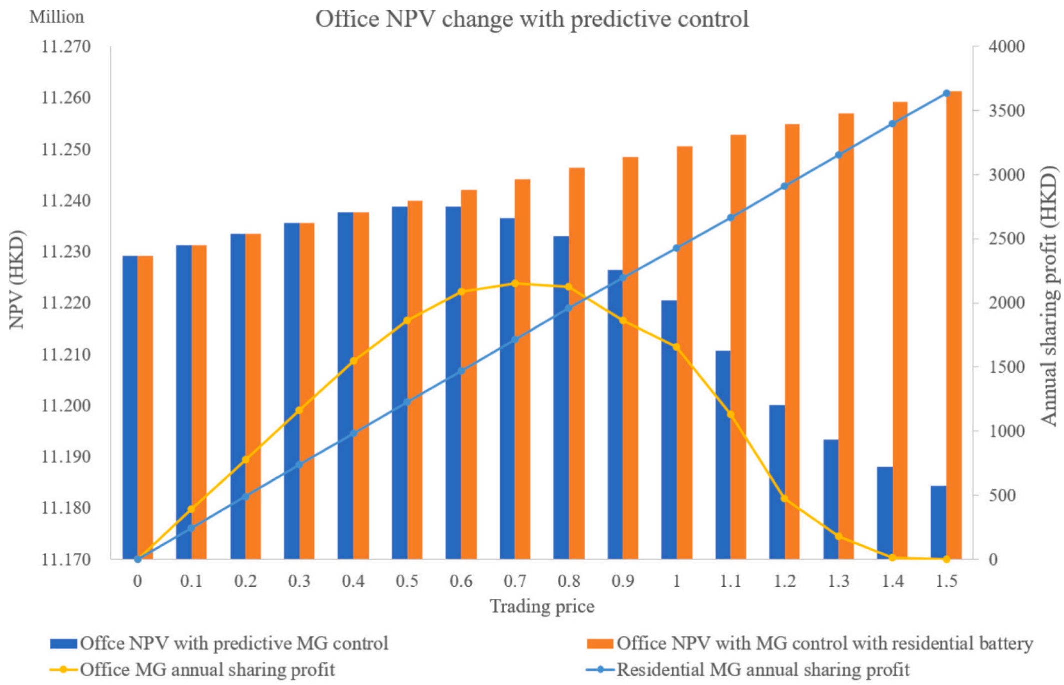

(a)

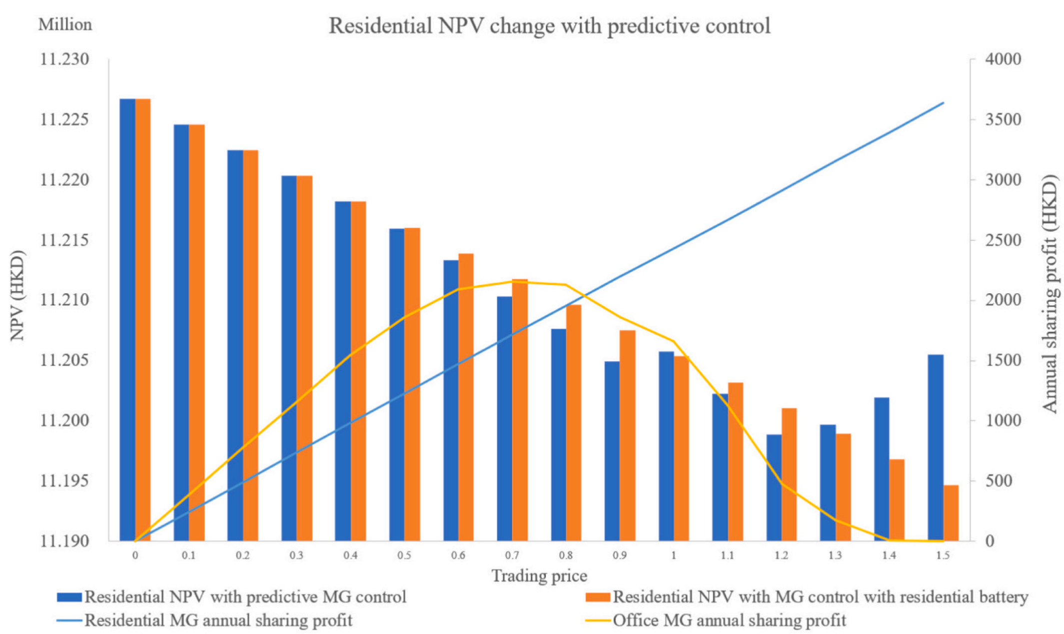

(b)

Fig. 15. Two buildings' NPV comparison with and without predictive control and residential annual sharing profit of micro-grid under different micro-grid trading prices. (a) Office building, and (b) Residential building.

strategy of EV sharing outlined in Section 3.2.3 remains consistent. The EV will charge or discharge whenever the parked building has a surplus or shortage. Two stakeholders make a mutual agreement for the trading price ranging from 0 to 1.5 HKD per kWh. The pattern of NPV changes under trading is similar to the micro-grid sharing first business model as presented by Case 5 in Fig. 12. Fig. 18 also indicates that the building sharing more energy with another building gets a higher NPV value as the trading price increases. Inversely, the NPV enlargement of this building becomes the subtraction part of another building's NPV without affecting the total NPV. In this business model, the building with more sharing gets extra benefits. It will be an interesting topic for future research to apply predictive sharing control to make the charging and discharging decision based on the future building energy conditions and trading price.

5.5. The comparison between different sharing methods

In this section, three aspects of three sharing methods (instantaneous

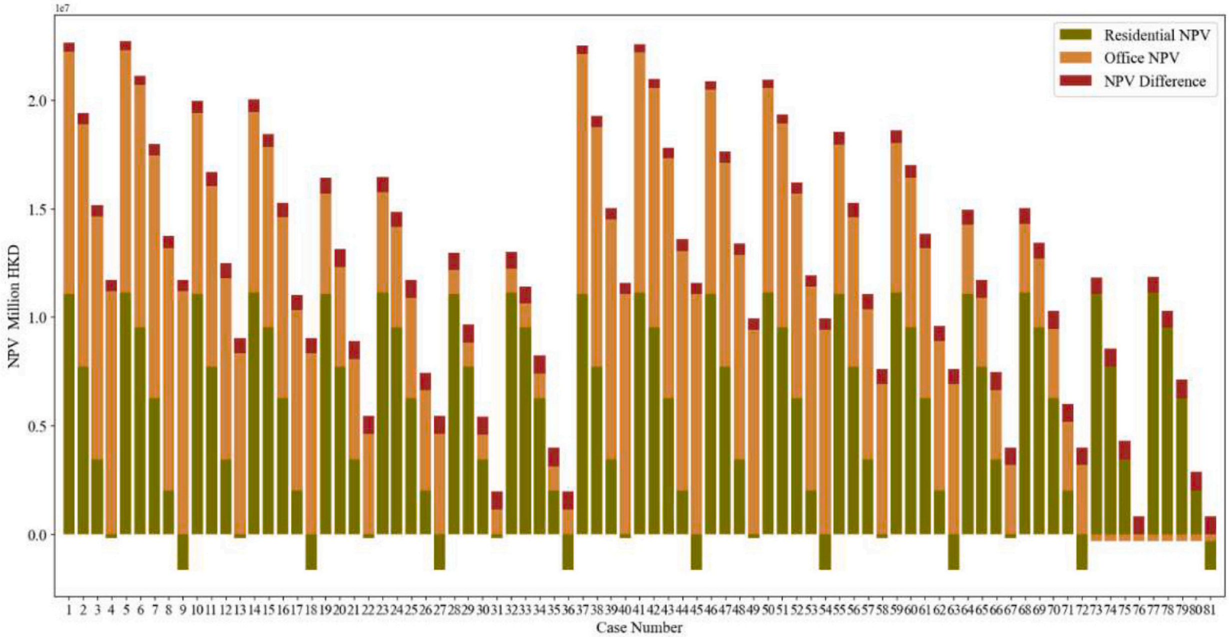

(a)

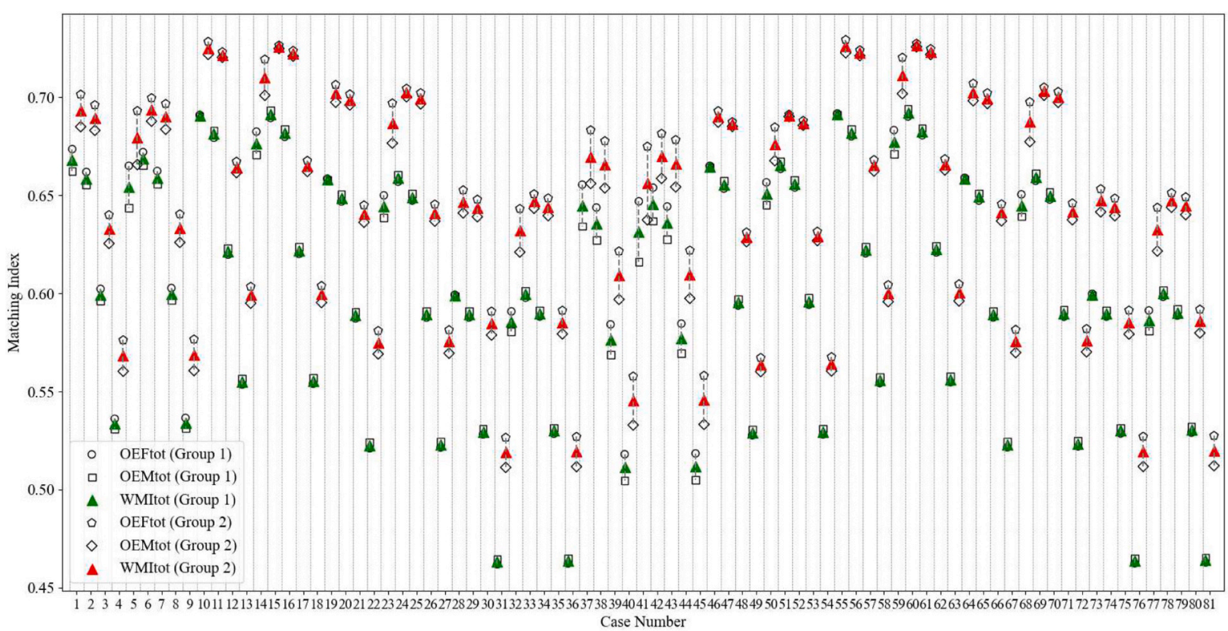

(b)

Fig. 16. The NPV and technical performance improvement with and without local EV-based sharing of all 81 combination cases in Group 4. (a) Total NPV improvement with and without local EV-based sharing of all 81 combination cases, and (b) Technical performance improvement with and without local EV-based sharing of all 81 combination cases.

micro-grid-based sharing, predictive micro-grid-based sharing and local electric-vehicle-based sharing) between these two neighboring buildings are compared. The first aspect is about the technical and economic performance, followed by the second aspect on the characteristics of energy sharing amounts, and the Feed-in Tariff (FiT) impact on NPV will be the last topic.

Firstly, compared to the reference case without any sharing, both instantaneous sharing methods bring a positive impact on the two buildings' system. As indicated in Table 16, the total WMI improvement of instantaneous micro-grid-based sharing and local EV-based sharing are 7.19 % and 6.86 % respectively, while the total NPV improvement is 9.53 % and 5.70 % respectively for these two methods. The degree of improvement on WMI and NPV varies with different combinations of two buildings. The instantaneity nature of micro-grid-based sharing results in significant improvement for two buildings with great diversity in renewables combinations, especially for the cases where one building is totally supported by PVs and another building supported by wind turbines, for example, Cases 45 and 40 in Table 12. These cases are the

Table 15
Top and worst 3 enhancement cases of total NPV and total WMI under Local EV-based sharing respectively in Group 4.

	Case number	Renewable combinations						Technical performance										Economic performance			
		Office			Residence			Office			Residence			Total				Office	Residence	Total	
		Number of BIPV	Number of FPV	Number of WT	Number of BIPV	Number of FPV	Number of WT	Office OEF	Office OEM	Office WMI	Residential OEF	Residential OEM	Residential WMI	Total OEF	Total OEM	Total WMI	Enhancement rate	Office NPV (HKD)	Residence NPV (HKD)	Total NPV (HKD)	Enhancement value (HKD)
Top 3 WMI enhance-ment cases	31	235	1367	0	235	1396	0	0.614	0.579	0.597	0.440	0.444	0.442	0.526	0.511	0.519	12.02 %	1,809,485	−28,563	1,780,922	846,083
	36	235	1367	0	0	1601	0	0.614	0.579	0.597	0.441	0.445	0.443	0.527	0.512	0.519	12.02 %	1,810,138	−1,465,015	345,123	846,544
	76	0	1572	0	235	1396	0	0.615	0.580	0.598	0.441	0.444	0.442	0.527	0.512	0.519	12.01 %	373,626	−26,703	346,923	846,600
Top 3 NPV enhance-ment cases	80	0	1572	0	0	1214	3	0.615	0.580	0.598	0.569	0.579	0.574	0.592	0.580	0.586	10.44 %	382,330	2,180,551	2,562,881	866,690
	35	235	1367	0	0	1214	3	0.614	0.579	0.597	0.568	0.579	0.574	0.591	0.579	0.585	10.44 %	1,817,951	2,178,679	3,996,631	865,924
	75	0	1572	0	235	1010	3	0.615	0.580	0.598	0.568	0.578	0.573	0.591	0.579	0.585	10.44 %	381,351	3,619,984	4,001,335	865,667
Worst 3 WMI enhance-ment cases	6	235	0	11	0	183	11	0.707	0.679	0.693	0.692	0.697	0.694	0.700	0.688	0.694	3.75 %	11,427,756	9,681,145	21,108,901	411,500
	1	235	0	11	235	0	11	0.708	0.679	0.693	0.695	0.691	0.693	0.701	0.685	0.693	3.78 %	11,434,478	11,220,574	22,655,052	416,311
	51	0	154	11	0	183	11	0.691	0.683	0.687	0.692	0.697	0.694	0.691	0.690	0.691	3.79 %	9,660,481	9,677,358	19,337,838	409,243
Worst 3 NPV enhance-ment cases	42	0	0	13	0	183	11	0.670	0.623	0.647	0.692	0.695	0.694	0.681	0.659	0.670	3.82 %	11,280,776	9,691,702	20,972,478	403,779
	41	0	0	13	0	0	13	0.669	0.624	0.647	0.680	0.651	0.666	0.675	0.637	0.656	3.91 %	11,274,320	11,309,929	22,584,249	407,415
	37	0	0	13	235	0	11	0.671	0.623	0.647	0.695	0.690	0.693	0.683	0.656	0.670	3.85 %	11,287,513	11,231,118	22,518,631	408,591
Average								0.689	0.672	0.685	0.605	0.607	0.606	0.651	0.639	0.645	6.86 %	6,646,402	5,662,263	12,308,664	664,295

top improvement cases on both technical and economic aspects. The mismatching generation profile between the two buildings creates the possibility of covering one's energy shortage with another's surplus through instantaneous micro-grid sharing. Moreover, the performance of the instantaneous micro-grid-based sharing is enhanced when the building is equipped with the building battery. The predictive micro-grid-based sharing results in a better economic outcome for residence under low trading price. Conversely, for the cases which both buildings with similar renewable proportions of PV and wind turbine combinations such as Cases 31 and 80 in Table 15, they achieve the top improvement on WMI and NPV values under the local EV-based sharing. The performance improvement level increases along with the similarity degree of renewable energy generation profile of each building. The energy allocation through the time-lag of EVs charging and discharging enables two buildings with similar generation profiles to have peak-shifting energy sharing ability which the micro-grid instantaneous sharing doesn't have. Inversely, the worst improvement cases on WMI and NPV of the two sharing methods follow the opposite logic as to the best improvement cases. The higher similarity in the two buildings' renewables portfolio causes poorer improvement in micro-grid-based sharing cases, while the lower similarity induces little enhancement in local EV-based sharing cases, as illustrated in Table 12 and Table 15. Therefore, the characteristics of two instantaneous sharing methods lead to different improvement results. Micro-grid-based sharing is better when two buildings have completely different renewable energy combinations, while local EV-based sharing is more efficient if the buildings share the same renewable portfolio. What's more, the residence NPV performance of Case 76 in Table 12 indicates that applying the micro-grid sharing may not guarantee a positive outcome for the stakeholder, considering the extra investment on the micro-grid itself exceeds the limited saved electricity bills. Instead, both stakeholders always benefit from applying the local EV-based sharing on account that there is no additional investment for it. It reveals that local EV sharing has the potential to improve economic performance only based on existing facilities without any further investment.

Secondly, different sharing methods show various trend of energy sharing amount magnitude. Under the instantaneous micro-grid-based sharing method, there is no significant difference between the average annual sharing amount from office to residence (8228 kWh) and the amount of the opposite direction (8127 kWh), but the two-way sharing values of each separate case are various depending on the renewable energy combinations. The renewable energy combination diversity affects the micro-grid sharing value as concluded in Section 5.2.1. The homogeneous combinations of two buildings result in lower sharing value since both buildings have high similarity in generation profile and there is less chance of energy surplus in one building and energy shortage in another building at the same time, for example, Case 76 in Table 12. Inversely, if the renewable combinations are diversified, the imparity of PV and wind turbine generation profiles gives more possibility for two buildings to utilize the other's surplus energy to compensate for their own shortage. Taking Case 45 in Table 12 as an example, the building with more wind turbine installed number transfers more energy to another building with more PV number due to the nature of night-time energy generation ability of wind turbine. Moreover, the surplus of PV generation in daytime is capable of compensating for the shortage in another buildings that wind turbines' generation cannot meet. These two factors lead to the larger amount of micro-grid energy sharing of the cases with higher diversity in renewable combinations. Moreover, under the predictive micro-grid-based sharing control, the sharing amount decreases with the increasing trading price, resulted from the DMI control strategy design. As to the local EV-based sharing, it is difficult to differentiate the actual transferring amount between two buildings in local EV-based sharing method, thus the sharing amount of local EV-based method cannot show the exact quantitative value but only represents qualitative comparison according to what has been mentioned in Section 4 and Section 5.4. Based on this

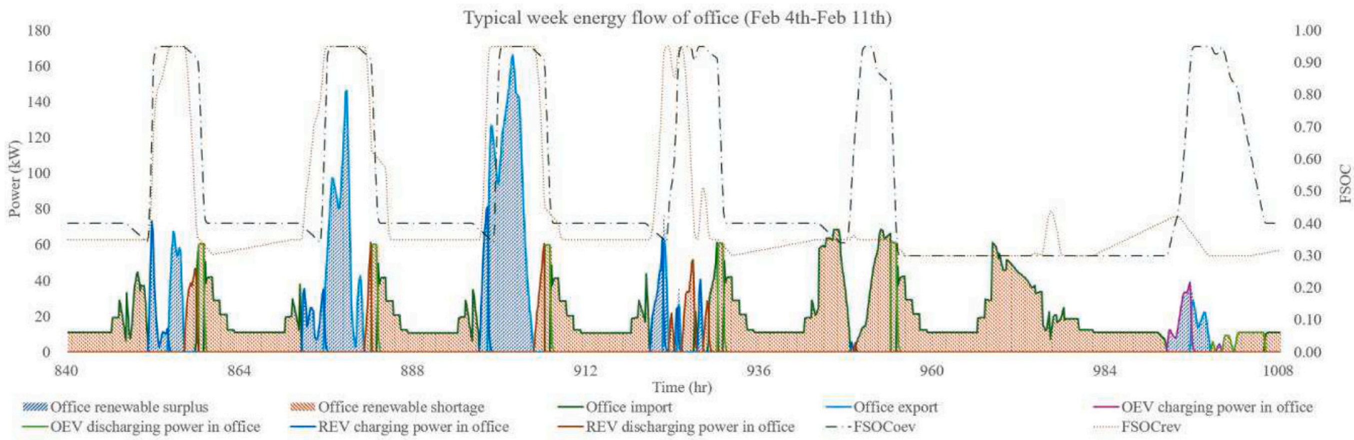

(a)

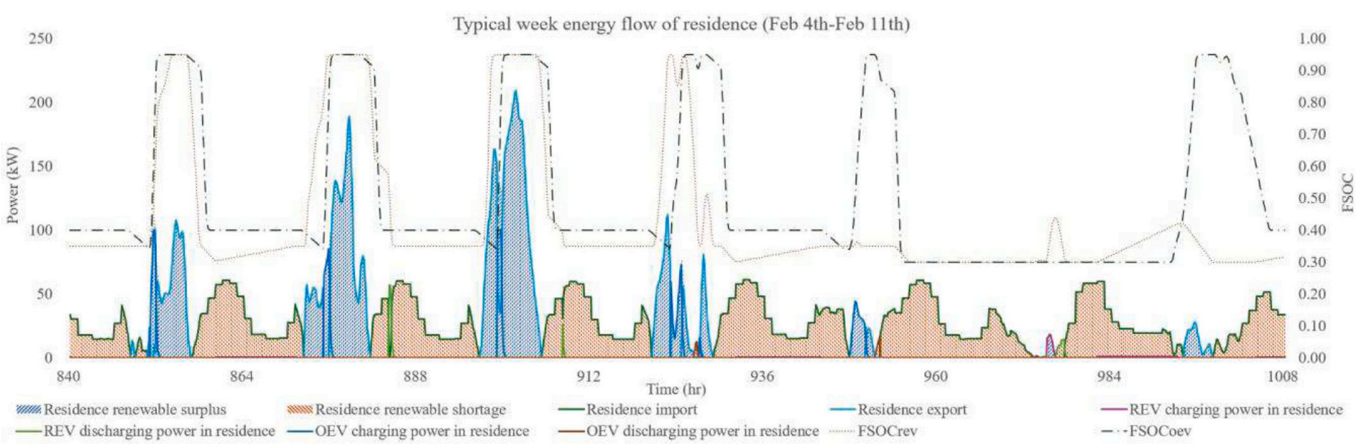

(b)

Fig. 17. Case 31: Typical week energy flow of two buildings from February 4th to February 11th. Time 840–864 means the first day (Monday) of the typical week. “OEV” and “REV” refer to the office EV and residential EV, respectively. (a) Office building, and (b) Residential building.

aspect, the simulation results show that the magnitude of average annual energy shared from residence to office is much higher than in the opposite direction. This feature comes from the characteristics of the energy demand profile of each building and the EV schedule. The active operation time of the office building is on weekday daytime, which happens to be the time that the residential EV parked in the office. At this time, the residential EV has been charged by the surplus energy the night before, therefore it is highly possible to have a high FSOC level and to discharge itself to fulfill the shortage of the office building. In another way, the time that the office EV is parked in the residence during daytime on weekdays is not the active period of the residential building, so the need for discharging the office EV to meet the residence demand is less. Unlike the micro-grid-based sharing that which direction has more energy transferred depending on the renewable combinations of each building, the residence-office transferred direction has a larger sharing amount in most cases under the local EV-based sharing method. Only few cases that the residence highly supported by PVs have similar two-way sharing amounts due to insufficient energy charged to the residential EV at night-time when it is parked in the residence.

Thirdly, the Feed-in Tariff policy sponsored by the Hong Kong government holds significant importance in evaluating the value of renewable energy investment. In Table 17, Case 1 is selected as the typical case to demonstrate the comparison results between four situations as mentioned in Table 9. Except for the reference case without any renewable energy systems, all combinations illustrated in Table 10 of Group 1 (without any sharing between each building as illustrated in Table 9) achieve positive NPV performance, except for one office renewable combination (Combination 9) and two residential renewable combinations (Combination 8 and 9). However, policies like FiT that compensate for every kWh generation of renewable energy systems are not commonly seen outside Hong Kong, so it is meaningful to study the impact of the FiT policy on the economic aspect. If the FiT policy is abolished, the NPV values of all the groups (Group 1 to 4) will become negative. The reference case, whose NPV is calculated based on the sum-up value of the interest-considered annual electricity bills for twenty years, obtains the worst economic performance among all groups. Case 1 of Group 1 without FiT compensation achieves a 29.6 % improvement in NPV compared to the reference case even with extra capital investment on PVs and wind turbines. This result means the renewables generation itself is capable of saving imported electricity and reducing the electricity bills. Regardless of the high capital investment, the saved electricity bills already bring attractive economic profits in the long-term aspect. As for Case 1 of Group 2 and 4, the application of two instantaneous sharing methods still has a similar improvement rate compared to Group 1, indicating that the sharing methods have the proximate enhancement efficiency on economic performance. Moreover, the differences of NPV improvement rate between two instantaneous sharing methods may vary depending on the renewable energy combinations as

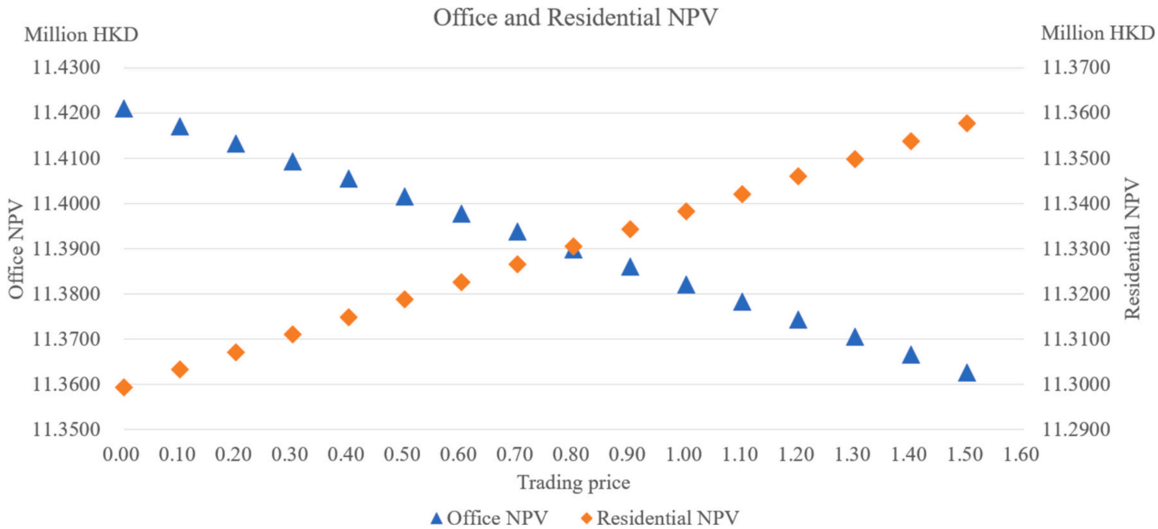

Fig. 18. Office and residential NPV change with trading price under local EV-based sharing.

abovementioned in the first paragraph in this section. It can be further concluded that it is worth investing in renewable energy systems even without the FiT policy, since the long-term benefits brought by the renewable energy already cover the investment of systems.

6. Conclusions

6.1. Conclusions of the research results

In pursuit of the decarbonization goal aiming for carbon neutrality before 2050, the building and transportation sectors emerge as crucial areas for attention. In this research, two neighboring buildings with different ownership, one office building and one residential building, that are supported by hybrid building-integrated photovoltaic (BIPV), floating photovoltaic (FPV) and wind turbine systems and integrated with one electric vehicle (EV) separately are studied. Three novel integrated energy-sharing methods, instantaneous and predictive micro-grid-based, and local EV-based sharing, are introduced to build energy-sharing connections between two buildings. Besides the trading price analysis on two instantaneous sharing methods, a special trading model based on the predictive control strategy has been introduced to regulate the energy sharing amount considering both trading price and future energy conditions under predictive micro-grid-based sharing. Extensive research has been conducted on the influence of various combinations of renewable energy sources, the interactions between two buildings employing three sharing methods, and the performance of the business models. The simulation results reveal several critical findings, which can be summarized as follows.

Firstly, while all the renewable energy combinations examined can enable these two buildings to achieve grid-tied net-zero-energy status, the technical and economic outcomes differ across the various mixes of renewable sources. A high proportion (from 7 to 11 units of wind turbines) of wind turbine generation leads to better technical performance with 14.52 % higher than the average WMI, while the cases with the number of wind turbines ranging from 11 to 13 achieve the best economic performance that are more than 90 % over than the average NPV. The mixed generation profile of a large proportion of wind turbines and a small proportion of PV shows better matching capability with two buildings' demand. However, the matching of the total PV-supported buildings is quite poor indicated by the WMI that is 23 % lower than the average WMI, therefore also resulting in poor economic performance, particularly for the full FPV-supported cases with 13,580,306 HKD less than the average NPV.

Secondly, by activating the instantaneous micro-grid-based sharing, the cable energy sharing shows positive enhancement of the matching capabilities indicated by the total WMI of all cases at the average level of 7.2 % improvement. The instantaneous micro-grid-based sharing also improves the NPV values of most cases except for few cases that the benefits brought by the technical improvement fail to compensate for the micro-electric cable investment. The cases with one building supported solely by wind turbines and another supported only by PVs have the largest energy-sharing amount and achieve the best enhancement up to 33.59 % of WMI and 3,764,380 HKD of NPV improvement. On the contrary, the cases with similar proportions of renewable energy are hard to share large amount of energy therefore the enhancement on technical and economic is limited. The results also indicate that with additional residential building battery under instantaneous micro-grid-based sharing, the residence shows significant technical and economic improvement while the office suffers from minor deterioration of matching capabilities and worse NPV performance as indicated by three typical selected cases. When predictive micro-grid-based sharing control is applied, the residential stakeholders can have positive financial enhancement when the trading price is not within the middle range. As for the energy trading by instantaneous micro-grid sharing, the building with more energy transferred by micro-grid earns more profits. Moreover, the optimal trading price under the predictive micro-grid-based sharing control of the typical selected Case 5 is below 0.5 HKD to realize the highest possibility for an acceptable mutual agreement between two stakeholders.

Thirdly, in the case the local EV-based sharing method is activated, a similar positive enhancement of an average 6.86 % improvement on total WMI can be observed. Unlike the micro-grid-based sharing requires investment on micro-electric cable, the local EV-based sharing utilizes the existing EVs and requires no further investment, thus the NPV values of all cases are improved at the average of 5.70 %. The cases that both buildings are supported by PVs can have the largest enhancement up to 12.02 % of total WMI, while the cases with the office building entirely supported by PVs and the residence supported by a large proportion of PVs and a small proportion of wind turbines achieve the best enhancement of NPV up to 866,690 HKD. On the flip side, an elevated proportion of wind turbine renewable energy translates to limited improvements in both WMI and NPV. On the aspect of energy trading, residential stakeholder earns the most profits due to the larger sharing amount from residence to office in most cases, except for few cases with a high PV portion renewable energy system. The performance of local EV sharing is highly related to the EV parking schedule, therefore the conclusions of local EV sharing may differ with various EV parking schedules.

Fourthly, as for the comparison between these three sharing methods, both instantaneous sharing controls bring positive impact on technical and economic aspects, apart from very few cases that have mentioned above under micro-grid-based sharing, while the local EV sharing always yield financial profits for stakeholders. Another predictive micro-grid-based sharing control deteriorates the technical performance when trading price gets higher, and only bring positive financial feedback for the residential stakeholder when trading price is within optimal range. Different renewable energy combinations lead to different enhancement results for different sharing methods. A larger diversity of renewable energy combinations contributes to a higher energy-sharing amount and brings better enhancement under micro-grid-based sharing method but little enhancement under the local EV-based sharing method. In contrast, high homogenization of renewable energy combination causes a large amount of sharing to happen under local EV-based sharing and links to greater enhancement but resulting in limited improvements under micro-grid-based sharing. Furthermore, the renewable energy system shows a positive attractiveness of investing even without the Feed-in Tariff sponsorship for both sharing methods.

Table 16
Technical and economic comparison of two instantaneous sharing methods.

Sharing method		Technical performance										Economic performance			
		Office			Residence			Total				Office	Residence	Total	
		Office OEF	Office OEM	Office WMI	Residential OEF	Resid-ential OEM	Resid-ential WMI	Total OEF	Total OEM	Total WMI	Enhan-cement rate	Office NPV (HKD)	Resident-ial NPV (HKD)	Total NPV (HKD)	Enhancement value (HKD)
Average	Instantaneous Micro-grid-based	0.686	0.677	0.682	0.611	0.615	0.613	0.648	0.646	0.647	7.19 %	6,875,112	5,878,860	12,753,972	1,109,602
	Local EV-based	0.698	0.672	0.685	0.605	0.607	0.606	0.651	0.639	0.645	6.86 %	6,646,402	5,662,263	12,308,664	664,295

6.2. Recommendations and general transferable ability of research outcome

The research results demonstrate a useful methodology for coastal zero-energy building (ZEB) and micro-grid investors, designers and operators. It is recommended for the investors or designers to use on-shore wind turbines to cover as much energy demand of ZEB as possible, for wind turbines show a better matching capabilities of building's demand and a shorter investment payback period. As for the renewable energy combinations setting, the investors should pay attention to the diversified energy demand pattern of different types of buildings and is advised to choose those renewable resources that its generation can better match the building demands. When it comes to the operator to choose which sharing methods should be adopted for two neighboring buildings, the micro-grid-based sharing is recommended under the situation that the diversity of renewable energy of two buildings is significant, otherwise the EV-based sharing is more suitable for similar renewable combinations. Under any circumstances, applying EV-based sharing always brings positive impact on both technical and economic aspects since the discharging process only has limited influence on the cycle number of EV battery. The operators should also be aware that the annual profit amount of sharing energy when trading price is applied under instantaneous sharing, or to have a mutual-agreement with another operator on a low trading price under predictive micro-grid-based sharing.

This research is conducted based on the environmental and policy background of Hong Kong. When the location of the studied buildings is in other regions of the world, the differences of environmental condition and policies may have impact on renewable energy and financial performance. For example, in European Union where the yearly solar fluxes are not as strong as Hong Kong, extra period for the PV investment financial payback can be expected. The selection of the renewable energy types should be carefully analyzed based on on-site renewable energy sources and local installation and operational cost. Secondly, this research adopts the electricity price 1.5440 HKD per kWh of Hong Kong, limiting the maximum trading price between two buildings. However, the electricity price in European Union compared to Hong Kong is much higher, therefore providing a larger space for better potential trading profits, resulting in a more active sharing motivation for the building operators. Thirdly, the Feed-in Tariff policy is a key element when calculating the investment profits. If other regions' governments provide a higher FiT policy, it is more likely to attract the investors to invest on renewable energy. Furthermore, the conclusion of the impact by various characteristics of different renewable energy combinations on diverse energy-sharing methods can also be a useful guide to other regions of the world.

Table 17
The comparison of different FiT applications.

Case 1		Office (HKD)	Relative NPV (HKD)	%	Residential (HKD)	Relative NPV (HKD)	%	Total (HKD)	Relative NPV (HKD)	%
REF	NPV without REW	−13,726,495	0		−13,974,029	0		−27,700,524	0	
G1	NPV without sharing and FiT	9,915,816	23,642,311	REF1	9,791,560	23,765,589	REF1	19,707,376	47,407,900	REF1
	NPV without sharing no FiT	−9,663,387	4,063,108	REF2	−9,787,643	4,186,386	REF2	−19,451,029	8,249,495	REF2
G2	NPV with micro-grid and FiT	10,063,730	23,790,225	1.5 % (Compared to REF1)	9,910,791	23,884,820	1.2 % (Compared to REF1)	19,974,521	47,675,045	1.4 % (Compared to REF1)
	NPV with micro-grid no FiT	−9,515,473	4,211,022	1.5 % (Compared to REF2)	−9,668,412	4,305,617	1.2 % (Compared to REF2)	−19,183,885	8,516,639	1.4 % (Compared to REF2)
G4	NPV with local EV sharing and FiT	10,167,496	23,893,991	2.5 % (Compared to REF1)	9,952,854	23,926,883	1.6 % (Compared to REF1)	20,120,350	47,820,874	2.1 % (Compared to REF1)
	NPV with local EV sharing no FiT	−9,411,707	4,314,788	2.6 % (Compared to REF2)	−9,626,349	4,347,680	1.6 % (Compared to REF2)	−19,038,056	8,662,468	2.1 % (Compared to REF2)

CRediT authorship contribution statement

Suijie Liu: Writing – review & editing, Writing – original draft, Methodology, Investigation. **Sunliang Cao:** Writing – review & editing, Writing – original draft, Supervision, Project administration, Methodology, Investigation, Funding acquisition, Conceptualization.

Declaration of competing interest

The authors declare that they have no known competing financial interests or personal relationships that could have appeared to influence the work reported in this paper.

Acknowledgements

This research is partially supported by the HK RGC (Hong Kong Research Grants Council) Research Project 15211822. This research is also partially supported by the Projects “P0043916” and “P0044567” from the Research Institute for Smart Energy (RISE), The Hong Kong Polytechnic University.

Appendix A

The setting parameters of the studied building envelopes, insulations and service systems are presented in Table 18

Table 18
The setting parameters of the studied building envelopes, insulations and service systems.

	Parameters	Values
Insulation (U-value, $W/m^2.K$)[(a)]	External roof	0.346
	External wall	0.239
	Ground floor layer	0.295
	Window glazing	2.780
Infiltration (h^{-1})[(a)]		According to the guideline of the Performance-based Building Energy Code of Hong Kong [40] When the ventilation is on, the infiltration is 0 h^{-1}; When the ventilation if off, the infiltration is 0.31 h^{-1}
Occupants	Number	31 occupants in each office floor 16 occupants in each residence floor
Ventilation, AHU cooling and AHU heating	Ventilation type[(a)]	Mechanical supply and exhaust ventilation with return air mixing and heat recovery
	Total supply flow rate (h^{-1})	3 h^{-1} for office (When the fan is on) 2 h^{-1} for residence (When the fan is on)
	Ventilation schedule	As listed in [40] for the ventilation schedule
	AHU cooling method[(a)]	7/12 °C cooling coil
	AHU heating method[(a)]	Electric heating
	Sensible effectiveness of the heat recovery device[(a)]	0.70
	Specific ventilation fan power ($W/(m^3/s)$)[(a)]	Supply fan: 800 Exhaust fan: 800
Space cooling[(a)]	Type	13/15 °C hydronic chilled ceiling system
	Room air set point (°C)	25 °C for all thermal zones
	Cooling schedule	As listed in [40] for the cooling schedule
Space heating[(a)]	Type	Electric heating

(continued on next page)

Table 18 (*continued*)

	Parameters	Values
DHW heating[(a)]	Room air set point (°C)	21 °C for all thermal zones
	Heating schedule	As listed in [40] for the heating schedule
	Set point (°C)	60
	Daily consumption volume (m^3)	3.30 m^3
	DHW Schedule	As listed in the [40] for the DHW schedule

(a) If the specific value of each building is not mentioned, the mentioned values are equal for both buildings.

Data availability

Data will be made available on request.

References

[1] Electrical & Mechanical Services Department (EMSD). The government of the Hong Kong special administrative region. Hong Kong Energy End-use Data 2023. Issue in September; 2023. [Online] Available. https://www.emsd.gov.hk/filemanager/en/content_762/HKEEUD2023.pdf.

[2] Environment Protection Department. The government of the Hong Kong special administrative region. Hong Kong's Climate Action Plan 2050. October 2021. [Online] Available. https://www.eeb.gov.hk/sites/default/files/pdf/cap_2050_en.pdf.

[3] Galvin R. Net-zero-energy buildings or zero-carbon energy systems? How best to decarbonize Germany's thermally inefficient 1950s-1970s-era apartments. J Build Eng 2022;54:104671.

[4] Heidari M, Rahdar MH, Dutta A, Nasiri F. An energy retrofit roadmap to net-zero energy and carbon footprint for single-family houses in Canada. J Build Eng 2022;60:105141.

[5] Xiang X, Ma M, Ma X, Chen L, Cai W, Feng W, et al. Historical decarbonization of global commercial building operations in the 21st century. Appl Energy 2022;322:119401.

[6] Wang Z, Shen H, Deng G, Liu X, Wang D. Measured performance of energy efficiency measures for zero-energy retrofitting in residential buildings. J Build Eng 2024;91:109545.

[7] Ahmed A, Ge T, Peng J, Yan W-C, Tee BT, You S. Assessment of the renewable energy generation towards net-zero energy buildings: a review. Energ Buildings 2022;256:111755.

[8] Li Y, Kumar GMS, Cao S, Wang S. Electric vehicle-based distant energy sharing between zero-emission coastal office and hotel buildings. J Build Eng 2024;90:109496.

[9] Han S, Yuan Y, He M, Zhao Z, Xu B, Chen D, et al. A novel day-ahead scheduling model to unlock hydropower flexibility limited by vibration zones in hydropower-variable renewable energy hybrid system. Appl Energy 2024;356:122379.

[10] Allouhi A, Rehman S, Buker MS, Said Z. Up-to-date literature review on solar PV systems: technology progress, market status and R&D. J Clean Prod 2022;362:132339.

[11] Olabi AG, Abdelkareem MA. Renewable energy and climate change. Renew Sust Energ Rev 2022;158:112111.

[12] Şirin C, Goggins J, Hajdukiewicz M. A review on building-integrated photovoltaic/thermal systems for green buildings. Appl Therm Eng 2023;229:120607.

[13] Zhou S, Cao S, Wang S. Realisation of a coastal zero-emission office building with the support of hybrid ocean thermal, floating photovoltaics, and tidal stream generators. Energy Convers Manag 2022;253:115135.

[14] Luo J, Joybari MM, Ma Y, Liu J, Lai K. Assessment of renewable power generation applied in homestay hotels: energy and cost-benefit considering dynamic occupancy rates and reservation prices. J Build Eng 2024;87:109074.

[15] Eze F, Ogola J, Kivindu R, Egbo M, Obi C. Technical and economic feasibility assessment of hybrid renewable energy system at Kenyan institutional building: a case study. Sustain Energy Technol Assess 2022;51:101939.

[16] Luo H, Cao S, Lu VL. The techno-economic feasibility of a coastal zero-energy hotel building supported by the hybrid wind–wave energy system. Sustain Energy, Grids Netw 2022;30:100650.

[17] Gao Q, Bechlenberg A, Jayawardhana B, Ertugrul N, Vakis AI, Ding B. Techno-economic assessment of offshore wind and hybrid wind–wave farms with energy storage systems. Renew Sust Energ Rev 2024;192:114263.

[18] Liu J, Chen X, Yang H, Shan K. Hybrid renewable energy applications in zero-energy buildings and communities integrating battery and hydrogen vehicle storage. Appl Energy 2021;290:116733.

[19] Luo J, Cao X, Yuan Y. Comprehensive techno-economic performance assessment of PV-building-EV integrated energy system concerning V2B impacts on both building energy consumers and EV owners. J Build Eng 2024;87:109075.

[20] Abdou N, Mghouchi YE, Hamdaoui S, Asri NE, Mouqallid M. Multi-objective optimization of passive energy efficiency measures for net-zero energy building in Morocco. Build Environ 2021;204:108141.

[21] Krarti M, Aldubyan M. Role of energy efficiency and distributed renewable energy in designing carbon neutral residential buildings and communities: case study of Saudi Arabia. Energ Buildings 2021;250:111309.

[22] Tumminia G, Sergi F, Aloisio D, Longo S, Cusenza MA, Guarino F, et al. Towards an integrated design of renewable electricity generation and storage systems for NZEB use: a parametric analysis. J Build Eng 2021;44:103288.

[23] Mo T, Lau K, Li Y, Poon C, Wu Y, Chu PK, et al. Commercialization of electric vehicles in Hong Kong. Energies 2022;15:942.

[24] Gilleran M, Bonnema E, Woods J, Mishra P, Doebber I, Hunter C, et al. Impact of electric vehicle charging on the power demand of retail buildings. Adv Appl Energy 2021;4:100062.

[25] Bracco S, Fresia M. Energy Management System for the Optimal Operation of a Grid-Connected Building with Renewables and an Electric Delivery Vehicle. IEEE EUROCON 2023 - 20th Int Conf Smart Technol. 2023. 00:472–7.

[26] Liu Q, Li Y, Xu T, Qian F, Meng H, Yao Y, et al. Peak shaving potential and its economic feasibility analysis of V2B mode. J Build Eng 2024;90:109271.

[27] Ouammi A. Peak load reduction with a solar PV-based smart microgrid and vehicle-to-building (V2B) concept. Sustain Energy Technol Assess 2021;44:101027.

[28] Liu J, Wu H, Huang H, Yang H. Renewable energy design and optimization for a net-zero energy building integrating electric vehicles and battery storage considering grid flexibility. Energy Convers Manag 2023;298:117768.

[29] Zou W, Sun Y, Gao D, Zhang X, Liu J. A review on integration of surging plug-in electric vehicles charging in energy-flexible buildings: impacts analysis, collaborative management technologies, and future perspective. Appl Energy 2023;331:120393.

[30] Borge-Diez D, Icaza D, Açıkkalp E, Amaris H. Combined vehicle to building (V2B) and vehicle to home (V2H) strategy to increase electric vehicle market share. Energy 2021;237:121608.

[31] Lo K-Y, Yeoh JH, Hsieh I-YL. Towards nearly zero-energy buildings: smart energy Management of Vehicle-to-Building (V2B) strategy and renewable energy sources. Sustain Cities Soc 2023;99:104941.

[32] He Z, Khazaei J, Freihaut JD. Optimal integration of vehicle to building (V2B) and building to vehicle (B2V) technologies for commercial buildings. Sustain Energy, Grids Netw 2022;32:100921.

[33] Ghafoori M, Abdallah M, Kim S. Electricity peak shaving for commercial buildings using machine learning and vehicle to building (V2B) system. Appl Energy 2023;340:121052.

[34] Huang P, Lovati M, Zhang X, Bales C, Hallbeck S, Becker A, et al. Transforming a residential building cluster into electricity prosumers in Sweden: optimal design of a coupled PV-heat pump-thermal storage-electric vehicle system. Appl Energy 2019;255:113864.

[35] Barone G, Buonomano A, Forzano C, Giuzio GF, Palombo A, Russo G. Energy virtual networks based on electric vehicles for sustainable buildings: system modelling for comparative energy and economic analyses. Energy 2022;242:122931.

[36] Cao S. The impact of electric vehicles and mobile boundary expansions on the realization of zero-emission office buildings. Appl Energy 2019;251:113347.

[37] Kumari A, Sukharamwala UC, Tanwar S, Raboaca MS, Alqahtani F, Tolba A, et al. Blockchain-based peer-to-peer Transactive energy management scheme for smart grid system. Sensors 2022;22:4826. https://doi.org/10.3390/s22134826.

[38] Kumari A, Shukla A, Gupta R, Tanwar S, Tyagi S, Kumar N. ET-DeaL: A P2P Smart Contract-based Secure Energy Trading Scheme for Smart Grid Systems. IEEE INFOCOM 2020 - IEEE Conf Comput Commun Work (INFOCOM WKSHPS). 2020. https://doi.org/10.1109/infocomwkshps50562.2020.9162989. 00:1051–6.

[39] Júnior SM, Frandoloso MAL, Brião VB. Technical and economic feasibility study for a university zero energy building in southern Brazil. Energ Buildings 2023;281:112748.

[40] Electrical & Mechanical Services Department (EMSD) The government of the Hong Kong special administrative region. Performance-based Building Energy Code 2007. 6.2-6.3 (P9-11), Appendix I (P21), Appendix III (P24-33) [Online] Available: https://www.emsd.gov.hk/filemanager/en/content_724/pb-bec_2007.pdf.

[41] Hong Kong green building council (HKGBC). Hong Kong Green Office Guide, 2016. [Online] Available, https://www.hkgbc.org.hk/eng/gog.aspx.

[42] Tesla Motors. Model S. 2023. [Online] Available, https://www.tesla.com/zh_hk/models.

[43] Recurrent. Tesla Model S. Recurrent Motors, USA, 2023. [Online] Available, https://www.recurrentauto.com/guides/tesla-model-s.

[44] Solar Energy Laboratory of the University of Wisconsin-Madison. TRANSSOLAR Energietechnik GmbH, CSTB – Centre Scientifique et Technique du Bâtiment, TESS–Thermal Energy Systems Specialists. Volume 4 Mathematical Reference of the standard types of the TRNSYS document package. 2018.

[45] FuturaSun. FU 275 P. [Online] Available, https://www.futurasun.com/wp-content/uploads/2019/12/2020_FuturaSun_60p_260-285W_en.pdf?x97762.

[46] TESS – Thermal Energy Systems Specialists, LLC of Madison. Wisconsin, USA. Section 3.6 Type 567: Glazed Building-Integrated PV System (Interacts w/ Type

56). Volume 03 Electrical Library Mathematical Reference of the TESSLibs Document Package. 2013. 71–88.
[47] Intelligentliving. Commercial-scale floating solar projects in open seas under development. [Online] Available. https://www.intelligentliving.co/commercial-scalefloating-solar-projects/; 2021.
[48] Statkraft. Statkraft selects norwegian ocean sun to supply floating solar plant in Albania. [Online] Available. https://www.statkraft.com/newsroom/news-and-stories/archive/2019/floating-solar-pv/; 2019.
[49] Chengdu Eagle Tech Energy Co.,Ltd. ET-WT10KL-W. [Online] Available, https://eagletechenergy.en.made-in-china.com/product/UqOndlZKQsro/China-10kw-Home-Use-Wind-Turbine-Wind-Power-Generator-System-10KW-Wind-Solar-Hybrid-System-Small-Wind-Power.html.
[50] Cao S, Hasan A, Sirén K. On-site energy matching indices for buildings with energy conversion, storage and hybrid grid connections. Energ Buildings 2013;64:423–38.
[51] Cao S, Hasan A, Sirén K. Matching analysis for on-site hybrid renewable energy systems of office buildings with extended indices. Appl Energy 2014;113:230–47.
[52] The Government of the Hong Kong Special Administrative Region. Scheme of Control Agreements (SCAs). [Online] Available, https://www.gov.hk/en/residents/environment/sustainable/renewable/feedintariff.htm.
[53] CLP,2023. Tariff2023_FAQ_ENG.pdf. [Online] Available, https://www.clp.com.hk/content/dam/clphk/documents/tariff-adjustment-20221/Tariff2023_FAQ_ENG.pdf.
[54] IRENA. Renewable Power Generation Costs in 2019. [Online] Available, https://www.irena.org/publications/2020/Jun/Renewable-Power-Costs-in-2019.
[55] B. P, Martins, "Techno-economic evaluation of a floating PV system for a wastewater treatment facility," 2019. [Online]. Available, https://kth.diva-portal.orgsmash/getdiva2:1332527/FULLTEXT01.pdf.
[56] The World Bank. Real interest rate (%)-Hong Kong SAR, China. [Online] Available, https://data.worldbank.org/indicator/FR.INR.RINR?end=2019&locations=HK&start=2010&view=chart.
[57] The World Bank.Official exchange rate (LCU per US$, period average)-Hong Kong SAR, China. [Online] Available, https://data.worldbank.org/indicator/PA.NUS.FCRF?end=2019&locations=HK&start=2011.